



UNIVERSITEIT VAN PRETORIA
UNIVERSITY OF PRETORIA
YUNIBESITHI YA PRETORIA

**THE LINK BETWEEN DAILY RAINFALL AND
SATELLITE RADAR BACKSCATTER DATA FROM THE ERS-2
SCATTEROMETER IN THE FREE STATE PROVINCE, SOUTH AFRICA.**

DIRK F. BOON

93272741

RESEARCH REPORT IN PARTIAL FULFILMENT OF
THE M.A. ENVIRONMENT AND SOCIETY

2004

DEPARTMENT OF GEOGRAPHY, GEOINFORMATICS AND METEOROLOGY
UNIVERSITY OF PRETORIA

SUMMARY

Radar backscatter intensity data from the ERS-1 and ERS-2 scatterometers are compared with daily rainfall data in two areas in the Free State province of South Africa. Knowledge of the relation between daily rainfall data and ERS C-band scatterometer data for a specific area can be useful to make reliable soil moisture measurements. The assumption is made that an increase in rainfall will lead to higher radar backscatter data values. This is based on the fact that moisture increases the dielectric properties of surfaces. This leads to higher backscatter intensities when incident radar energy is reflected back to the sensor.

Various techniques are used to study the relationship between daily rainfall data and ERS scatterometer data. It includes correlations, interpolations, visual interpretations, statistical analysis, and a simple model.

Weak positive correlations were found between radar and rainfall data in arid areas. This is supported by literature regarding the Sahel. No correlation was found in agricultural areas receiving more rainfall. Vegetation also increases radar backscatter intensities, even in the absence of rain. There is thus a relationship between rainfall and radar data but it is more visible in arid areas and over longer periods of time.



TABLE OF CONTENTS

SUMMARY	2
TABLE OF CONTENTS	3
LIST OF FIGURES AND TABLES	4
LIST OF APPENDICES	5
ACKNOWLEDGEMENTS.....	6
1. Introduction	7
1.1 Context and background	7
1.2 Problem description	8
1.3 Research objective(s).....	8
2. Literature Review	8
2.1 Basic theory of radar remote sensing.....	8
3. Data Types and their Analysis	13
3.1 Radar data	13
3.2 Rainfall data.....	14
3.3 Ancillary data.....	14
4. The Study Areas	14
5. Data Analysis and Results	15
5.1 General data exploration	15
5.1.1 Looking at the WSC database	15
5.1.2 Rainfall interpolation maps.....	17
5.1.3 Correlation between monthly NRCS intensity values and monthly rainfall	18
5.2 Specific cases.....	19
5.2.1 Meteorological stations in selected pixels.....	19
5.2.2 Rainfall data in comparison to NRCS intensity values	21
5.2.3 Local rainfall variation.....	24
5.2.4 Months of highest and lowest rainfall / NRCS intensity values.....	24
5.2.5 Modelling NRCS intensity values with daily rainfall data.....	26
6. Discussion	31
7. Conclusion.....	34
REFERENCES	35
LIST OF APPENDICES	Error! Bookmark not defined.
POWERPOINT TIME SEQUENCES.....	Error! Bookmark not defined.

LIST OF FIGURES AND TABLES

Figure 2.1: The electromagnetic wavelength spectrum (from: Lillesand & Kiefer, 2000:5).....	9
Figure 2.2: The Side Looking Radar system (from: Lillesand & Kiefer, 2000:620).....	10
Table 1: Different microwave band designations and wavelengths (from Lillesand and Kiefer, 2000:637).....	11
Figure 2.3: Radar reflection from various surfaces (from: Lillesand & Kiefer, 2000:646).....	11
Figure 2.4: X-band and L-band reflection from surfaces of varying roughness (from: Lillesand & Kiefer, 2000:648).....	12
Figure 3.1: Daily rainfall data in text format (source: South African Weather Service, 2003).	14
Figure 5.1: Average backscatter per pixel from August '91 to August '99 (source: ESA, 2001; data manipulation: WSC database application).	16
Figure 5.2: Average backscatter per pixel for South Africa for December 1998 (source: ESA, 2001; data manipulation: WSC database application).....	17
Figure 5.3: Location of radar pixels from the WSC database (pixels are numbered from top left to bottom right; sources: ESA, 2001; South African Weather Service, 2003; data manipulation: ArcView GIS software).	20
Figure 5.4: Meteorological stations selected per pixel in two areas of the Free State (Area 1 and Area 2; sources: ESA, 2001; South African Weather Service, 2003; data manipulation: ArcView GIS software).	20
Figure 5.5: Average monthly rainfall and monthly NRCS intensity values for Rietfontein (pixel 5; sources: ESA, 2001; South African Weather Service, 2003; data manipulation: MS Excel).	22
Figure 5.6: Average monthly rainfall and monthly NRCS intensity values for Williamstrip (pixel 11; sources: ESA, 2001; South African Weather Service, 2003; data manipulation: MS Excel).	23
Figure 5.7: Positive correlation: average 3-month NRCS intensity values and average 3-month rainfall (sources: ESA, 2001; South African Weather Service, 2003; data manipulation: MS Excel).	24
Figure 5.8: Rainfall at meteorological station Rust and its neighbours within various WSC database pixels (rainfall in mm; sources: ESA, 2001; South African Weather Service, 2003; data manipulation: ArcView GIS software).	25
Figure 5.9: Months of highest and lowest rainfall and NRCS (pixels 1 to 8; sources: ESA, 2001; South African Weather Service, 2003; data manipulation: MS Excel).	25
Figure 5.10: Months of highest and lowest rainfall and NRCS (pixels 9 to 17; sources: ESA, 2001; South African Weather Service, 2003; data manipulation: MS Excel).	26
Figure 5.11: Rainfall events for meteorological station at Petra in November 1998 (source: South African Weather Service, 2003; data manipulation: MS Excel).	27
Figure 5.12: Comparison of total rainfall, weighted NRCS intensity values and real NRCS intensity values, meteorological station at Petra (sources: ESA, 2001; South African Weather Service, 2003; data manipulation: MS Excel).....	30

LIST OF APPENDICES

- APPENDIX 1:** Interface designed to work with scatterometer data (source: ESA, 2001; data manipulation: WSC database application).**Error! Bookmark not defined.**
- APPENDIX 2:** Meteorological stations in the Free State (source: South African Weather Service, 2003; data manipulation: ArcView GIS software).....**Error! Bookmark not defined.**
- APPENDIX 3:** Annual precipitation rates for the Free State (source: ENPAT, 2000a).....**Error! Bookmark not defined.**
- APPENDIX 4:** Land cover types in the Free State (source: ENPAT, 2000b). **Error! Bookmark not defined.**
- APPENDIX 5:** Time series of NRCS intensity values in box around the Free State province (source: ESA, 2001; data manipulation: WSC database application).....**Error! Bookmark not defined.**
- APPENDIX 6:** Rainfall map of the Free State on 1 November 1998 (source: South African Weather Service, 2003; data manipulation: ArcView GIS software).**Error! Bookmark not defined.**
- APPENDIX 7:** Comparisons of monthly rainfall (in mm; x-axis) and monthly NRCS intensity values (in dB; y-axis) (sources: South African Weather Service, 2003; ESA, 2001; data manipulation: MS Excel).**Error! Bookmark not defined.**
- APPENDIX 8:** Daily rainfall variations in relation to pixel size (source: South African Weather Service, 2003; data manipulation: ArcView GIS software).....**Error! Bookmark not defined.**
- APPENDIX 9:** Daily rainfall patterns per month for meteorological station at Petra (source: South African Weather Service, 2003; data manipulation: MS Excel). ...**Error! Bookmark not defined.**

ACKNOWLEDGEMENTS

Many thanks to the following people:

- Dr. Ingrid Stengel (University of Pretoria) for her indispensable ideas, comments and guidance in this research project.
- Dr. Dirk Hoekman and especially Dr. Peter van Oevelen (Wageningen University and Research Centre) for their professional support and education in Radar Remote Sensing.
- The Centre for International Students (with Vinay Rajah as director) and the University of Pretoria for financial support to study GIS and Remote Sensing abroad.
- Tracey Gill (South African Weather Service) for providing the necessary meteorological data of the Free State province in South Africa.
- Marian for her indispensable support, love and care.
- All family members and friends, far away or in close proximity, for their support.

Most thanks to our faithful and almighty God who cares for all of us – people, animals, trees, the whole earth ... every day.

1. Introduction

1.1 Context and background

The growing global population leads to an increased pressure on agriculture as key food producer. Increasing importance of not only high-yield, but also sustainable and ecologically sensitive agriculture in especially developing countries, on a national and regional basis, makes it necessary to study the natural parameters that are essential in agriculture. One of the most important factors for reliable agricultural production is the soil water budget. Optimum soil moisture levels will ensure the presence of good conditions for the growth of agricultural vegetation. Soil moisture is not only a crucial and limiting factor in terms of crop yield or failure, but is also closely related to and interdependent of surface runoff, water retention capacity of different soils, the intensity of evaporation of a given area and the near-surface microclimate. The correct assessment and monitoring of soil moisture is thus an extremely important task and relates to a whole range of agricultural, environmental and morphodynamic applications (Wagner, 1998; Woodhouse. & Hoekman, n.d.).

The accurate estimation of soil moisture, however, has been an expensive and labour-intensive task so far, as it has to be done on the ground itself (Wagner, 1998). Methods and tools to alleviate the costs and facilitate the procedure would be highly welcomed. Remote Sensing (RS) is a useful tool to solve this problem, as large areas can be monitored within a short period of time when soil moisture is calculated – provided suitable RS sensor and resolution types are selected for the analysis. Although field data still remain indispensable, even with RS methods, the cost and scale related to the calculation of soil moisture in the field might be reduced considerably. This study focuses on the applicability of data from the European ERS-1 and ERS-2 satellites (ERS = European Remote-Sensing Satellite). Both satellites carry a wind scatterometer originally designed for the measurement of wind speeds over the oceans (Johannessen et al., 2000). What is of much more importance for this research objective, in addition to the scatterometer, is that the ERS sensor provides a wealth of high temporal resolution radar backscatter intensity data over land surfaces as well (Frison et al., 1998; Boogaard et al., 2000) which can be used in the measurement of soil moisture over large areas.

The research approach is based on the fact that, rather than average annual or monthly precipitation figures, it is the *daily rainfall* which is the most determining single factor when estimating the soil moisture. The more precipitation, the higher the soil moisture will be for a specific area and time. The more variable the precipitation is on a daily basis, the more dramatic will be the effect on the soil moisture content fluctuations. Other factors, of course, are the amount of sunshine hours, cloudiness, air humidity, temperature, soil type and land cover type. In general, the knowledge of the relation between daily rainfall data and ERS C-

band scatterometer data for a specific area can be very useful to make reliable soil moisture measurements.

1.2 Problem description

High soil moisture levels in the topsoil layer result in high radar backscatter intensities (Hoekman & van Oevelen, 2002). This is due to the fact that soil moisture increases the dielectric properties of land surfaces (refer to Chapter 2). As with increasing rainfall, the soil moisture of a specific land surface will increase. One can assume that this will result in higher backscatter intensity values for a specific area. But what is the relation or link between rainfall and radar backscatter for a specific area and time? It is important to know this relation when using rainfall and ERS scatterometer data in the measurement of soil moisture for a specific area and time.

1.3 Research objective(s)

The research objective is to investigate the link between daily rainfall data and ERS C-band scatterometer data in the Free State province (South Africa) for a 3-monthly period between 1 November 1998 and 31 January 1999.

2. Literature Review

2.1 Basic theory of radar remote sensing

This overview of the theory of radar remote sensing provides the information on the concepts and processes that are related to this study. For more detail on the theory of radar remote sensing, see Lillesand & Kiefer (2000) and Hoekman & van Oevelen (2002).

Remote Sensing is “the science and art of obtaining information about an object, area, or phenomenon through the analysis of data acquired by a device that is not in contact with the object, area, or phenomenon under investigation” (Lillesand & Kiefer, 2000:1). Although the reading process with one’s eyes doesn’t really fit part of this definition (a human eye is not a device but an organ), the reading process is a good illustration of how the remote sensing process works. Just as your eye is not physically attached to this paper when you read these words, so does a satellite move around the earth in a fixed orbit and collect data about the earth with different sensors without being attached to the earth itself.

Optical remote sensors, on the one hand, measure the amount of (sun)light (electromagnetic energy) reflected by the earth’s surface. They are called passive remote sensing systems as they do not illuminate the earth with their own source of energy, but detect the reflected light from another source (the sun), or the emitted energy from the earth itself. These systems measure electromagnetic energy from the visible part of the electromagnetic spectrum to the thermal infrared part. An important drawback of these systems is the fact that

clouds, haze, vapour and darkness (night) block the sight on the earth in these parts of the electromagnetic spectrum (Lillesand & Kiefer, 2000). Refer to Fig 2.1 for the location of the optical (visible and infrared light) and microwave remote sensing locations on the electromagnetic spectrum.

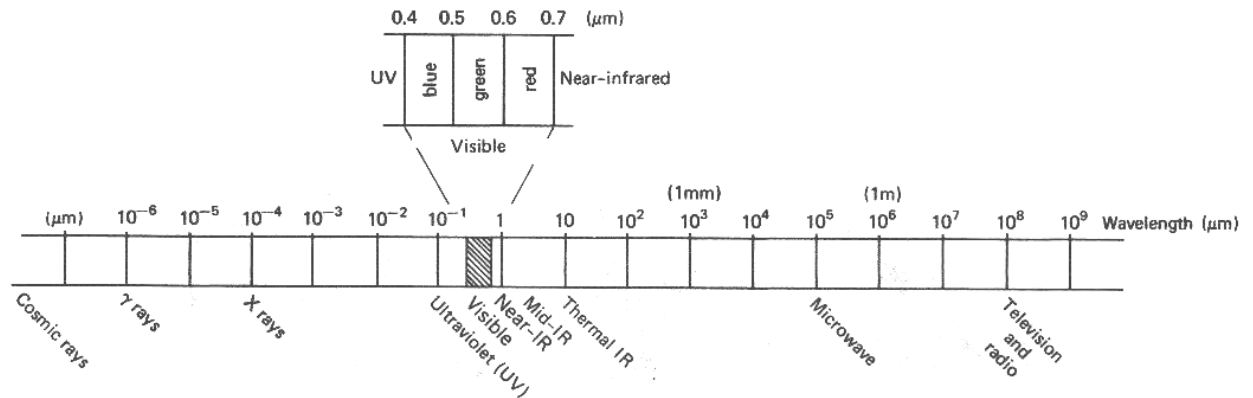


Figure 2.1: The electromagnetic wavelength spectrum (from: Lillesand & Kiefer, 2000:5).

Radar remote sensors, on the other hand, detect electromagnetic energy in the microwave part of the spectrum. Usually they are so-called active systems, illuminating the earth with their own source of energy (except microwave radiometry where the limited microwave emission from the earth is measured) (Hoekman & van Oevelen, 2002). The best-known advantage of these systems (depending on wavelengths used, see below) is that they can “see” through clouds and can work at night. The scatterometers on board the ERS are active systems too.

Radar stands for ‘radio detection and ranging’ (Hoekman & van Oevelen, 2002). As used at airports (to detect the positions and distances of aircraft), satellite-mounted radar antennae transmit short pulses of microwave energy in the direction of the area of interest. The strength of the “echoed” energy is measured in dB (decibels) and this reflected signal could be used to describe the area that was illuminated. An equivalent in nature is the way in which bats navigate their way through darkness. Fig. 2.2 illustrates this process in the case of side-looking radar (SLR), a principle used by nearly all satellite radar systems. If they were nadir-looking (directly downward), “echoed” signals from the left or right of the flight path of the satellite could not be distinguished from each other because they would reach the antenna at exactly the same time.

The ground resolution of a SLR radar system depends on two parameters: (i) The shorter the *pulse length* (the time taken to emit one pulse of energy), the better the spatial resolution because more objects on the earth surface that are “in front of each other” can separately be detected; this is called the range resolution, in the direction of the emitted energy. (ii) The smaller the *width of the antenna beam*, the better the spatial resolution

because more objects on the earth surface that are “next to each other” can separately be detected; this is called the azimuth resolution, in the direction of satellite movement.

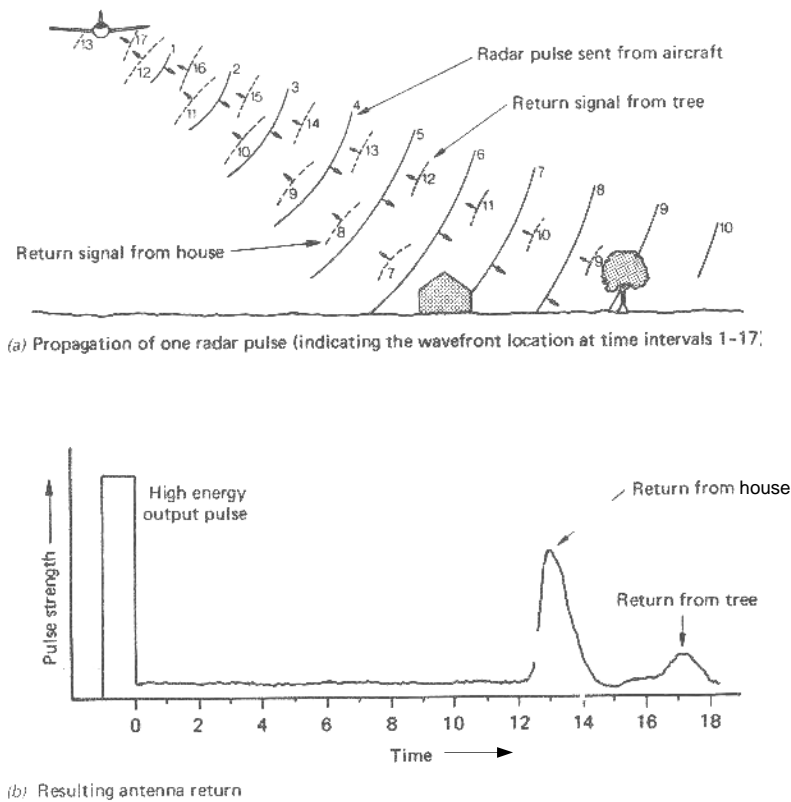


Figure 2.2: The Side Looking Radar system (from: Lillesand & Kiefer, 2000:620).

Radar signals of different wavelengths are used to study the earth surface. Table 1 provides a list of the different band designations and their associated wavelengths. A surface with irregularities in the magnitude of more or less 5 cm will look like a flat surface when illuminated with microwaves with a wavelength of 20 cm (L-band). The same surface will have a rough look when illuminated with wavelengths of 5 cm (C-band). Also refer to Fig. 2.4.

Table 1: Different microwave band designations and wavelengths (from Lillesand and Kiefer, 2000:637).

Radar Band Designations		
Band Designation	Wavelength λ (cm)	Frequency $\nu = c\lambda^{-1}$ [MHz (10^6 cycles sec^{-1})]
K_u	0.75–1.1	40,000–26,500
K	1.1–1.67	26,500–18,000
K_u	1.67–2.4	18,000–12,500
X	2.4–3.75	12,500–8,000
C	3.75–7.5	8000–4000
S	7.5–15	4000–2000
L	15–30	2000–1000
P	30–100	1000–300

Microwaves of all wavelengths can be transmitted and received in different modes of polarization, either in horizontal (H) and/or vertical (V) wave forms (perpendicular to the direction of propagation) (Hoekman & van Oevelen, 2002; Lillesand & Kiefer, 2000). An HH like-polarized system will transmit waves horizontally and receive the “echoes” back horizontally. A VV like-polarized system will transmit waves vertically and receive the “echoes” back vertically. Cross-polarized systems look like this: HV or VH. Some advanced systems can synthesize waves anywhere between the vertical and horizontal plane.

The polarization is important as different surfaces of the earth will react differently to polarized microwaves. A C-band VV system will receive strong “echoes” (also called backscatter) from an agricultural land where the stems of all the plants are positioned vertically upwards (Hoekman & van Oevelen, 2002). This will not be the case with a C-band HH system. Different polarizations can thus be used to study different phenomena on the earth surface.

When interpreting radar signals, it must be kept in mind that the geometric and dielectric properties of the earth’s surfaces under study will have the largest influence on the received signal strength. Figures 2.3 and 2.4 illustrate the effect of geometric properties.

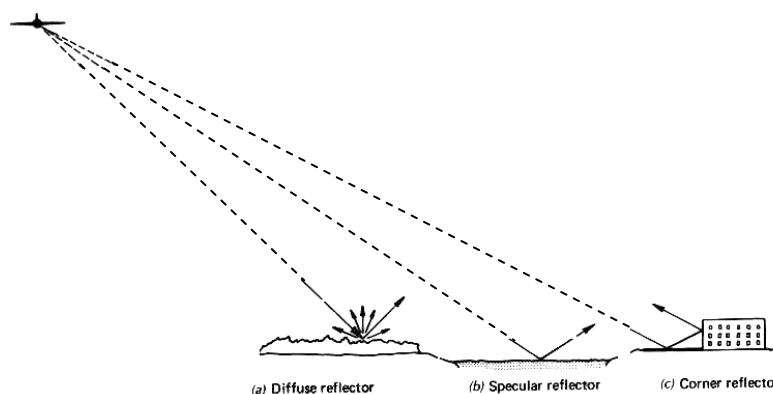


Figure 2.3: Radar reflection from various surfaces (from: Lillesand & Kiefer, 2000:646).

A diffuse reflector will result in a small return of backscatter to the sensor as most energy is diffusely scattered in all directions. A specular reflector, on the other hand, will return no backscatter to the sensor as everything is scattered away (like a mirror). Calm water, for example, can be an excellent specular reflector. A corner reflector will return the signal to the sensor although the object was not in a perpendicular position to the wave direction. A building next to a road can be an excellent corner reflector. A relatively flat object that is perpendicular to the direction of microwave propagation will return a lot of backscatter and will result in a strong backscatter intensity signal.

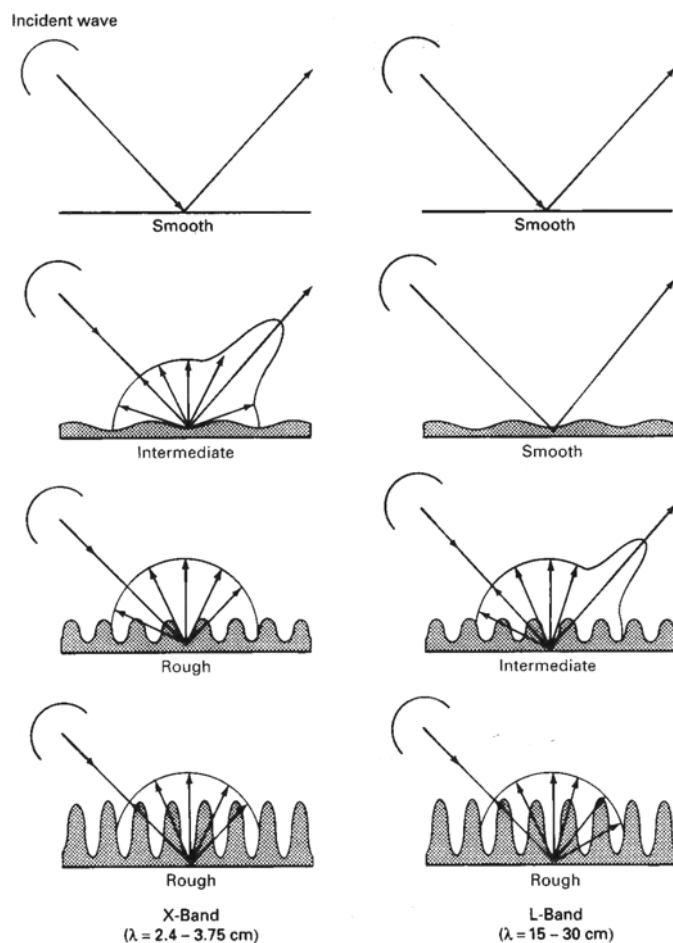


Figure 2.4: X-band and L-band reflection from surfaces of varying roughness (from: Lillesand & Kiefer, 2000:648).

The dielectric properties of materials on the earth surface relates to their reflectivity and conductivity. It is measured by the *complex dielectric constant*, a value describing the freedom that electrons in materials have to adjust their movement in accordance with the incident microwave energy and how they consequently increase or decrease the strength of the returned backscatter signal. Most dry natural materials have a dielectric constant of between 3 and 8, while water has one of 80. Metal is also known to have a very high dielectric constant. Electrons in metal can adjust freely to the incident microwave energy and

increase the returned radar backscatter signal. Water or moisture on a dry surface can significantly increase the dielectric constant of a material and increase the strength of the returned backscatter signal to the antenna. Plants also have a higher dielectric constant than dry soils as they contain moisture in their leaves.

In short one can summarize the above principles as follows: The geometric properties of a surface will determine where the radar backscatter will go while the dielectric properties will determine how much radar backscatter will be returned to the antenna.

3. Data Types and their Analysis

This chapter introduces the data types (radar, rainfall, and ancillary data) used for this research project and discusses their quality and methods of analysis.

3.1 Radar data

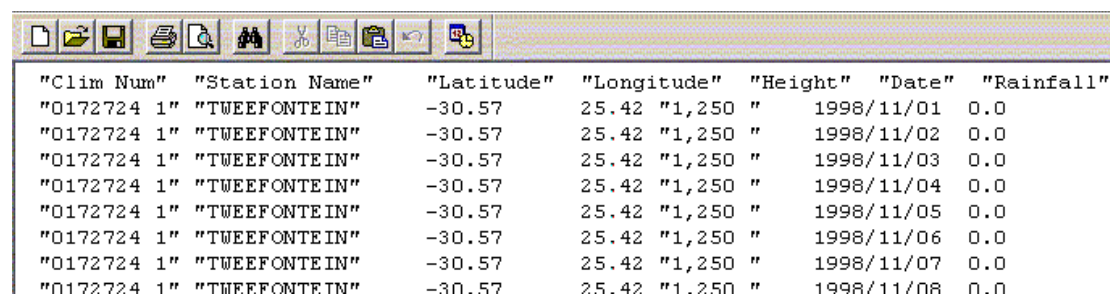
The ERS Wind Scatterometers are sensors on the European Remote-Sensing satellites (ERS-1 and ERS-2) (Wismann, 1999). They measure radar backscatter intensity (NRCS, Normalised Radar Cross Section) of the earth in the C band (5.3 GHz) with a VV polarisation. The scatterometers' three antennae look 45° forward, sideways and 45° backwards with respect to the satellite flight track. The swath width (width of area measured) is 500 km and the spatial resolution is 50 km. The scatterometer measures the backscatter coefficient σ^0 in dB. The strength of the signal mainly depends on the incidence angle, soil moisture content, surface roughness and vegetation biomass (Wagner et al., 1996). Thus a backscatter signal is a mix of many factors (Wagner, 1998): the dielectric properties of the surface (vegetation and soil), the vegetation density, the relative size of vegetation components with respect to the incident wavelength, as well as soil surface roughness. As the spatial resolution is very coarse, the surface roughness may vary within the pixel area and might thus not have a large influence on the overall radar backscatter signals. As shown above, the dielectric properties of vegetation and soils are closely linked to their moisture content (Frison et al., 1998). In general it is assumed that an increase in the dielectric properties of objects will result in an increase in backscatter (Hoekman & van Oevelen, 2002). Thus an increase in soil and vegetation moisture will result in higher backscatter intensities. It can therefore be assumed that rainfall will cause an increase in backscatter intensities because it increases soil and vegetation moisture.

A CD-ROM database, freely available from the European Space Agency (ESA, 2001) in Noordwijk, Holland, containing global backscatter intensity data derived from the ERS scatterometer (time span: Aug 1991 to Aug 1999), is used. This is called the WSC (Wind Scatterometer) database. The highest temporal resolution available on this CD-ROM is one

month: one backscatter intensity value per pixel per month. A special interface through IDL (Interactive Data Language software) is used to work with these data (Appendix 1).

3.2 Rainfall data

Daily rainfall data for the whole of the Free State province were obtained from the South African Weather Service (2003) in text format (Fig. 3.1) for the period between 1 November 1998 and 31 January 1999. These data were imported into MS Excel, where all columns were formatted to a specific data type. These formatted data were then saved as a Dbase file (*.dbf) and inserted into ArcView as a table. With the “add event theme” option, this table was inserted into a view using the correct columns for the latitude and longitude coordinates. The table was then converted into an ArcView shapefile (*.shp). This is a suitable format for querying the data and for making spatial analysis. Data like cloudiness, temperature and sunshine hours were also received, but they were not available for all meteorological stations, they were omitted for the purpose of the rest of this research.



"Clim Num"	"Station Name"	"Latitude"	"Longitude"	"Height"	"Date"	"Rainfall"
"0172724 1"	"TWEEFONTEIN"	-30.57	25.42 "1,250 "	1998/11/01	0.0	
"0172724 1"	"TWEEFONTEIN"	-30.57	25.42 "1,250 "	1998/11/02	0.0	
"0172724 1"	"TWEEFONTEIN"	-30.57	25.42 "1,250 "	1998/11/03	0.0	
"0172724 1"	"TWEEFONTEIN"	-30.57	25.42 "1,250 "	1998/11/04	0.0	
"0172724 1"	"TWEEFONTEIN"	-30.57	25.42 "1,250 "	1998/11/05	0.0	
"0172724 1"	"TWEEFONTEIN"	-30.57	25.42 "1,250 "	1998/11/06	0.0	
"0172724 1"	"TWEEFONTEIN"	-30.57	25.42 "1,250 "	1998/11/07	0.0	
"0172724 1"	"TWEEFONTEIN"	-30.57	25.42 "1,250 "	1998/11/08	0.0	

Figure 3.1: Daily rainfall data in text format (source: South African Weather Service, 2003).

3.3 Ancillary data

Data from the Digital Chart of the World (DCW, 1997) were downloaded as reference data to the meteorological stations, to provide a reference base for the daily rainfall point data. Only the following DCW data layers were used: Boundaries (international, provincial, administrative areas) and populated places. Appendix 2 shows an orientation map of the locations of all the meteorological stations in the study area.

4. The Study Areas

Two different areas were chosen for which rainfall data were compared to NRCS intensity values (Figures 5.3 & 5.4). Area No. 1 is located in the Free State province to the north of Lesotho where there are quite a number of densely spaced meteorological stations (Appendix 2). The spatial density of the meteorological stations was an important issue for the following reason. The pixel size of the WSC database is 50 km. The more meteorological stations in one pixel, the more accurate the comparison is expected to be between rainfall and NRCS intensity values. In Area No. 1, Bethlehem is one of the bigger towns. This area has

the highest annual precipitation rates of the province (Appendix 3). The main land cover type in this area is cultivated land (Appendix 4).

To compare rainfall data and NRCS intensity values in other areas and to provide a wider reference base, a second area was chosen. Area No. 2 is located in the southwest of the Free State province bordering the Eastern and Northern Cape provinces (Appendix 2). Being a semi-arid area, its annual precipitation is considerably lower than that of Area No. 1 (Appendix 3). The main land cover type in Area No. 2 is grassland and shrubland.

Due to their different characteristics, these study areas show different trends and variations in terms of rainfall and NRCS intensity values as will be discussed below.

5. Data Analysis and Results

To answer the research question, several types of analyses were carried out, both general and detailed, to obtain the necessary information. As the data analysis and the problems encountered therewith are also part of the results, both, the analysis and the results, are discussed in this chapter.

5.1 General data exploration

5.1.1 Looking at the WSC database

At first the data were surveyed in a general way to get an overall perspective of the data quality and extent. In the WSC database interface, a box was defined that includes the Free State province (see box in Appendix 1). The box's coordinates are UL^{*}: 24.39; -26.68; LR[†]: 29.61; -30.65.

A time series graph was made of the backscatter intensities through the time-span of the database of the area in this box (Aug 1991 to Aug 1999) (Appendix 5). The data are shown in 3-month periods. It is clear that the peak NRCS intensity values mostly occur at the end of each year suggesting high moisture conditions and/or an increase in vegetation density at that time of the year. The average backscatter intensity value for this box over the complete time span is -12.19 dB. In perspective: a very high backscatter intensity value for this database is about -7 dB, as would be found in a tropical area like Central Africa, South America (Amazon area) or Indonesia. A very low backscatter intensity value of e.g. -26 dB could be found in desert areas like the Sahara or the Arabian Peninsula. These values were extracted from the database.

From the standard deviation lines it is clear that, although some periods of low backscatter occur, backscatter intensities tend to have an inclination toward to the maximum backscatter intensity values; this suggest longer periods during which moisture is available to

* UL = Upper Left corner

† LR = Lower right corner

increase backscatter intensities. The difference between the maximum and minimum values is also not very large, a fact which indicates relative stable conditions on the surface that influenced the radar backscatter.

The trend value of 0.04 dB/a indicates a slow increase in average backscatter intensities per year in this box for the complete time-span of the database. This may indicate that conditions existed which slowly increased the backscatter intensities, e.g. higher soil moisture content or more vegetation perhaps due to more agricultural activities.

Although the maximum and minimum values are not very far apart, their pattern per year doesn't seem to be regular. When comparing the mean backscatter time line with the seasonal fit line, the irregular pattern of recurring maximum and minimum values may be due to irregular seasonal variations of rainfall or vegetation growth as is typical for a semi-arid area with high interannual and interseasonal variability.

A map of the average backscatter intensity values per pixel (box size same as above) for the time-span of the database (Aug 1991 to Aug 1999) is shown in Fig. 5.1. The main features in this map are that high backscatter intensities were recorded over Lesotho to the lower right of the box. Lower backscatter intensities occurred over the areas in the Free State province bordering the drier areas in the Northern and Eastern Cape provinces. The remainder of the area has medium backscatter intensities between these two extremes. There seem to be a link between the aridness and wetness of an area and backscatter intensities. The drier an area, the lower the backscatter intensities will be that occur over that area. It is assumed that high backscatter intensities over Lesotho are caused by high rainfall patterns in this mountainous country.

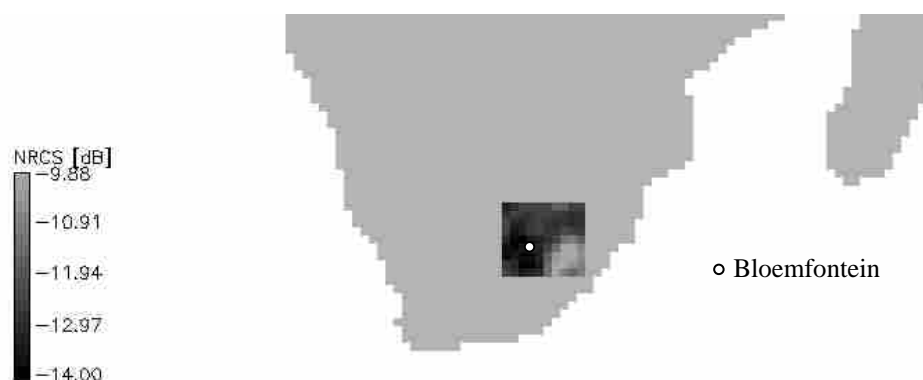


Figure 5.1: Average backscatter per pixel from August '91 to August '99 (source: ESA, 2001; data manipulation: WSC database application).

In Fig. 5.2, a map is shown of an area containing the whole of South Africa, but only for average backscatter intensities per pixel in the month of December 1998[‡]. The higher

[‡] Calculating average NRCS values for large areas as well as for the complete time-span of the database, takes quite some time, especially if the computer processor is not so large

backscatter intensities for the south and east coast up to the Limpopo Province are visible, extending westward into the Northwest Province. Also visible are the lower backscatter intensities for the northern parts of the Northern Cape province extending into the Kalahari Desert region and Namibia as well as those in the western parts of the Free State province. The area around Gauteng province shows relatively high backscatter intensities. This is partly due to the fact that man-made structures return relatively high backscatter intensities if they are aligned well in terms of the direction of outgoing radar signals (Chapter 2).

In general it can be concluded that there is a positive correlation between the moisture conditions in an area and its radar backscatter intensity.

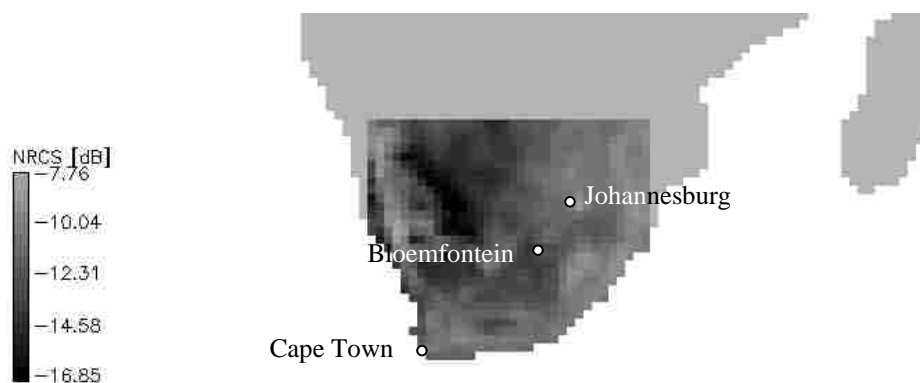


Figure 5.2: Average backscatter per pixel for South Africa for December 1998 (source: ESA, 2001; data manipulation: WSC database application).

5.1.2 Rainfall interpolation maps

In order to get a clear view of the daily rainfall in the Free State province, interpolation maps were made based on the daily rainfall data from each meteorological station (Appendix 2). There are 92 days in the period between the 1st of November 1998 and the 31st of January 1999. The interpolation method thus produced 92 maps. Not all of them can be shown here, please refer to the PowerPoint animation files on the cd accompanying this report (p. 45). In these presentations high rainfall situations at the borders of the province are not accurate due to various problems in the interpolation process. This is discussed below.

Appendix 6 shows the rainfall situation on the 1st of November in the Free State province. The interpolation (spline tension method, ArcView) process was limited to a certain pre-selected spatial extent. This is the reason why the rainfall estimation on the map does not stretch to the borders of the whole map. Furthermore it is important to realise that this is an interpolation and not an extrapolation. The estimation of rainfall is only reliable within the spatial limits of the outer points (meteorological stations) towards the central parts of the province. The estimations outside these boundaries are not based on reliable information from a meteorological station close-by, but from point values that are far away. The rainfall

estimation west of Kimberley is thus not accurate as it is based on the point information east and south of Kimberley.

The estimation of the rainfall inside the boundaries of the outer points (meteorological stations) is accurate (taking into account the scale of the maps), because the density of meteorological stations is high and they are well distributed over the area. A shortcoming is that the spread of the points is irregular. The rainfall estimation is thus more accurate on some places than on others due to the availability of more meteorological stations in that specific area. Small-scale differences in precipitation can however not be accounted for with these kind of interpolations. In most cases the meteorological stations are several kilometres apart. That is why this is an indication of the rainfall on a regional level only. South of Kroonstad, e.g., there are two meteorological stations very close to each other. Their distance from each other is however still 5.82 km. It is possible that it can rain in one place on a specific day, but 6 km away, it remains dry. A more specific case in this regard will be studied later.

Some general remarks can be made about the PowerPoint animations. In November the most precipitation occurred in the north-eastern parts of the Free State province while the south and south-western parts received little rain. The 1st, 8th, 17th and 18th of this month received a lot of rain. In December more widespread precipitation occurred in the whole province including the south and south-western parts. The northern parts still received the most precipitation. High precipitation rates occurred on the 15th, 17th – 20th, 29th and 30th of this month, although less when compared to November's top rainfall days. In January the same trend is visible as in December, also with relatively high rainfall in the south and south-western parts as well as widespread rain throughout the province. High precipitation rates occurred on the 4th, 10th, 20th, 22nd, 24th, 26th and 29th of this month. On the last two days high rainfall occurred at isolated places in the south of the province. January show more isolated rainfall peaks in terms of temporal location than November or December.

5.1.3 Correlation between monthly NRCS intensity values and monthly rainfall

The assumption was made that a high correlation will exist between monthly rainfall data and monthly NRCS intensity values of the pixels in which specific meteorological stations are located. This assumption is proven false when rainfall figures per month (from August '91 to August '99) and monthly NRCS intensity values are compared in a scatter graph. In Appendix 7, some scatter graphs are shown for various meteorological stations in pixels 4 and 10 (refer to Figures 5.3 and 5.4 for the location of these pixels).

It is clear from these graphs that monthly rainfall figures (X-axis) do not show a positive correlation with NRCS intensity values (Y-axis) – high monthly rainfall figures cannot be associated with high monthly NRCS intensity values. The relations seem to be very arbitrary. It is assumed that this non-correlation is due to other factors influencing NRCS

intensity values like vegetation growth and density as well as the local climate. It may also be due to local rainfall variation in pixels. Rainfall can show a lot of variation in a large area such as the area falling into one pixel (50 * 50 km). Furthermore, these are the correlations for only 6 meteorological stations in two selected pixels in the area. It may however be that other pixels show different (even more positive) correlation characteristics. Unfortunately time did not allow for the investigation of other pixels in this regard.

5.2 *Specific cases*

5.2.1 *Meteorological stations in selected pixels.*

Specific meteorological stations within specific pixels were chosen for a closer investigation in terms of the link between rainfall data and NRCS intensity values. More than one meteorological station was located in almost all selected pixels, because of the large pixel size of the WSC database (50 * 50 km). The data from these meteorological stations could provide much information about the variation of daily rainfall within the area of one pixel. There was however one problem: The geographical projection system (Goode Homolosine) used in the WSC database is different from the system used for the coordinates of the meteorological stations (based on the 1:50 000 topographical map reference system). Investigation into the geographical reference system of the radar data didn't come up with clear results (Wismann & Lin, 2003). To compensate for this uncertainty in location, only the meteorological stations that are more than 10 km away from the limits of a pixel and within the limits of a pixel were selected. This was to ensure that the meteorological stations are located within the right pixels to be able to compare the right rainfall and backscatter data with each other.

In a tedious manual process, the boundaries of 17 pixels were digitized in ArcView with the help of the WSC database interface. It was tedious because it is not possible to overlay the rainfall data in the WSC database application. It is also not possible to export the data from the WSC database into a more usable format (shape or grid file). The coordinates of the meteorological stations and those of other points were used to establish the boundaries of the radar pixels. Based on a quick estimation, no effort was made to specify the boundaries of a pixel if it did not contain any meteorological stations further than 10 km within its borders. Fig. 5.3 shows the locations of the pixels that were used as well as all the meteorological stations in the Free State. The pixels are numbered from top left to bottom right.

There are two areas that were studied – Area 1 just north of Lesotho and Area 2 in the south west of the province. These areas display quite different meteorological characteristics (Chapter 4). Fig. 5.4 zooms in to these two areas to show which meteorological stations were selected and used in each pixel. The selected meteorological stations are marked with a green dot.

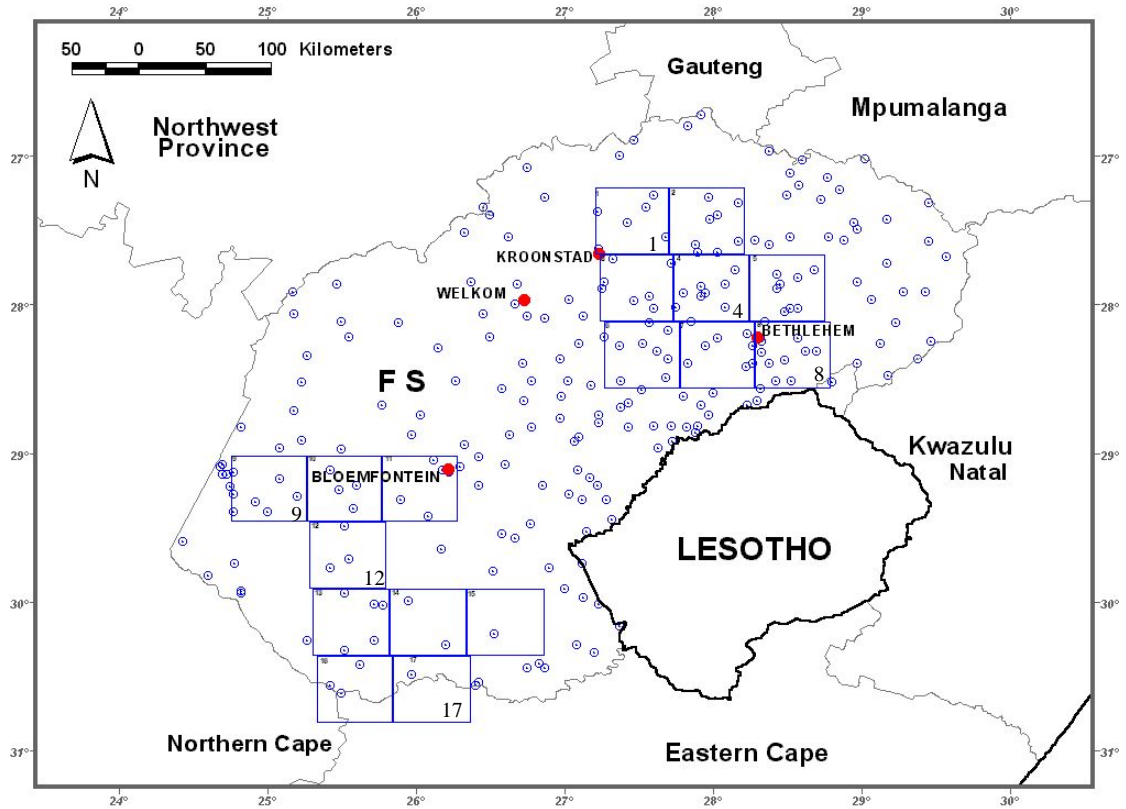


Figure 5.3: Location of radar pixels from the WSC database (pixels are numbered from top left to bottom right; sources: ESA, 2001; South African Weather Service, 2003; data manipulation: ArcView GIS software).

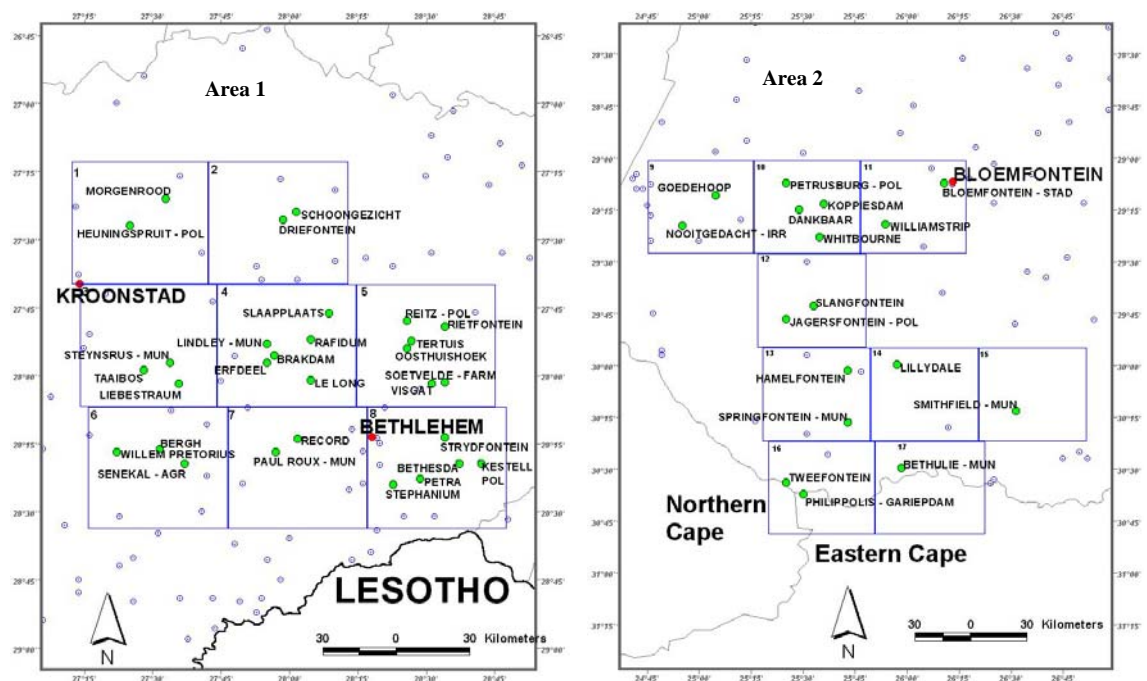


Figure 5.4: Meteorological stations selected per pixel in two areas of the Free State (Area 1 and Area 2; sources: ESA, 2001; South African Weather Service, 2003; data manipulation: ArcView GIS software).

5.2.2 Rainfall data in comparison to NRCS intensity values

The next step was to extract the daily rainfall data per meteorological station from the data files received from the South African Weather Service. They were ordered per month to make it easier to compare it with monthly NRCS intensity values. The NRCS intensity value per month per pixel was extracted as well. The average of the rainfall per month was calculated from each month's daily rainfall. This average value was then graphically compared with the monthly NRCS intensity value to see whether an increase in monthly rainfall can be associated with an increase in monthly NRCS intensity value.

Pixels 1 to 8 show a steady increase in monthly NRCS intensity values. An example is pixel 5: November '98: -12.78 dB; December '98: -12.22 dB; January '99: -11.8 dB. All pixels show the same pattern although the dB strength levels show some variation. There is quite some variation in the rainfall at the meteorological stations in these pixels. The general trend is that the highest rainfall occurs in December and the lowest in January. From the 28 meteorological stations in pixels 1 to 8 (not 29, Morgenrood had insufficient rainfall data, Fig. 5.4), ten meteorological stations displayed a different pattern. Schoongezicht (pixel 2), Steynsrus, Taaibos (pixel 3), Le Long (pixel 4), Bethesda, Kestell police station and Petra (pixel 8) had more rain in January than in December, but still the most in November. These exceptions only show a positive correlation between monthly rainfall and monthly NRCS intensity values for the months December and January. The meteorological stations in pixels 3 and 8 are also slightly clustered together suggesting that rainfall conditions may have been slightly different from the rest of the meteorological stations in that region. Brakdam and Erfdeel (pixel 4) had most of their rain in December and least in January. Willem Pretorius (pixel 6) had no data for November. These variations do not show a positive correlation between monthly rainfall and monthly NRCS intensity values.

The overall trend for pixels 1 to 8 can be summarised with Fig. 5.5 (Rietfontein, pixel 5) – an increase in monthly NRCS intensity values with a decrease in monthly rainfall. The conclusion is that there does not seem to be a positive correlation between monthly NRCS intensity values and monthly rainfall although some meteorological stations show a slight positive correlation for December and January.

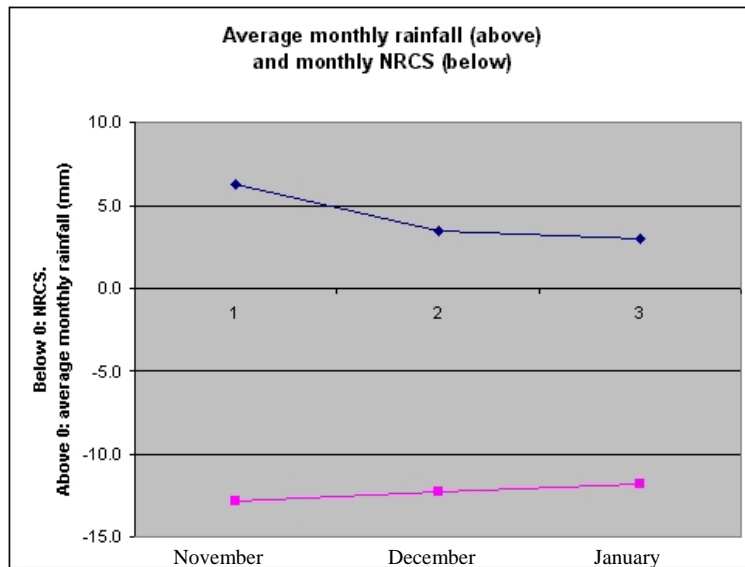


Figure 5.5: Average monthly rainfall and monthly NRCS intensity values for Rietfontein (pixel 5; sources: ESA, 2001; South African Weather Service, 2003; data manipulation: MS Excel).

In pixels 9 to 17 (Area 2), NRCS intensity values increase from November to December and decrease a little from December to January, or they decrease much towards January. The division between these two differences is about equal. This means that December has the highest monthly NRCS intensity values for all pixels. There is one exception (pixel 15) where December and January have the same NRCS intensity value. An example is pixel 13: November '98: -14.6 dB; December '98: -13.76 dB; January '99: -14.42 dB. Monthly rainfall data in these pixels show quite some variation but in general the opposite pattern of the NRCS intensity values is visible – with an increase in monthly NRCS intensity values, there is a decrease in monthly rainfall. A good example is Williamstrip in pixel 11 (Fig. 5.6).

In this area a strong positive correlation between monthly rainfall and monthly NRCS intensity values doesn't seem apparent. There are some exceptions, where a positive correlation is visible for the months December and January. In these cases a decrease in monthly rainfall results in a decrease in the monthly NRCS intensity values. They are Goedehoop (pixel 9), Dankbaar (pixel 10), Jagersfontein police station (pixel 12), Lillydale (pixel 14), Tweefontein (pixel 16) and Bethulie municipality (pixel 17). These exceptions are all quite well distributed with no explicit spatial connotation between them, also with respect to appendix 4 (land cover). They also constitute a large percentage of the total number of meteorological stations. More of a positive correlation can be seen for the two months December and January. This partial trend distinguishes Area 2 from Area 1.

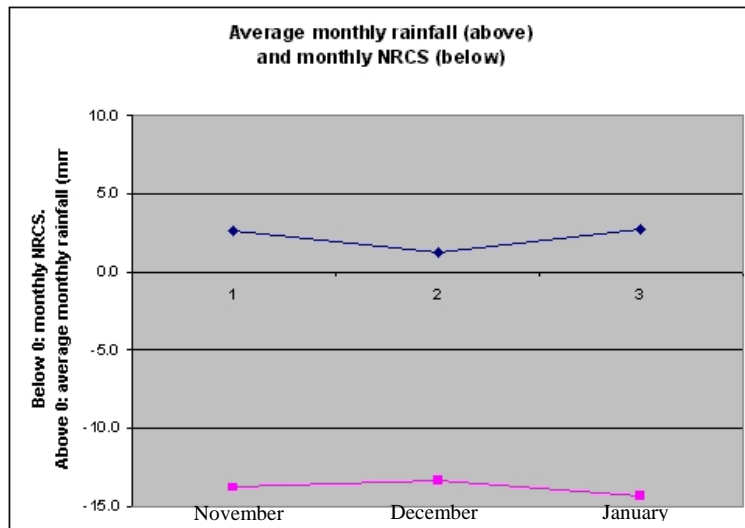


Figure 5.6: Average monthly rainfall and monthly NRCS intensity values for Williamstrip (pixel 11; sources: ESA, 2001; South African Weather Service, 2003; data manipulation: MS Excel).

In general it doesn't seem as if there is any strong positive correlation between monthly rainfall and monthly NRCS intensity values. It is interesting however that the average monthly NRCS intensity values as well as monthly rainfall figures are higher in Area 1 than in Area 2. The fact that pixels 9 to 17 (Area 2) are situated over a more arid environment than pixels 1 to 8 (Area 1; Appendices 3 and 4) seems to be true in this case when looking at NRCS intensity values and rainfall figures. Furthermore there is a positive correlation between the average rainfall for three months per meteorological station and the average NRCS intensity values for three months (Fig. 5.7, all selected meteorological stations were used). This suggests that a stronger correlation between rainfall and NRCS intensity values is found over longer terms.

According to Woodhouse and Hoekman (n.d.), there is a strong correlation between the monthly precipitation rates and the monthly NRCS intensity values at certain Sahel test sites. Frison (1998) and Jarlan (2002) found that in certain cases there is a strong relationship between yearly NRCS intensity values with yearly rainfall data in the Sahel (Mali). Frison and Jarlan support the suggestion that a stronger correlation may be found over longer periods. Woodhouse and Hoekman's results however only seem to be true for a small minority of meteorological stations in the Free State province of South Africa (Area 2) and then only for two months at most.

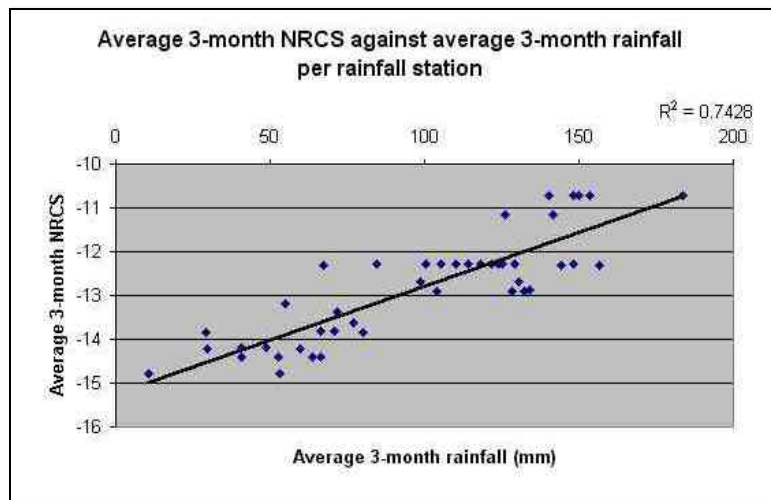


Figure 5.7: Positive correlation: average 3-month NRCS intensity values and average 3-month rainfall (sources: ESA, 2001; South African Weather Service, 2003; data manipulation: MS Excel).

5.2.3 Local rainfall variation

Daily rainfall shows considerable variations over small areas. Appendix 8 indicates how daily rainfall (29 December 1998) varies within the area of the WSC database pixels (50 * 50 km). Refer especially to pixel 6 (Fig. 5.8). The meteorological station at Rust received 67 mm of rain that day, while the meteorological stations surrounding it received little or no rainfall: Gordonia (0 mm), Bergh (7 mm), Senekal AGR (4.5 mm), Concordia (3.5 mm), De Echo (0 mm), Paul Roux Municipality (7 mm), Florida (0 mm), Roodepoort (0 mm) and Liebestraum (0 mm). The meteorological station farthest away from the station at Rust is De Echo (27.55 km) while the nearest meteorological station is at Gordonia (14 km). This indicates the high variation within an area that has the same size as one WSC database pixel. It is clear that the data in one pixel can only capture some of this daily variation if an NRCS intensity value of the area under study is derived very frequently (e.g. every hour). This is not possible as the revisit period of the ERS 1 and 2 satellites are 4 days at its most (for full resolution data).

5.2.4 Months of highest and lowest rainfall / NRCS intensity values

A comparison follows of the months with the highest and lowest NRCS intensity values and rainfall figures. For all the selected meteorological stations, divided in terms of Area 1 and Area 2 (Fig. 5.3), the months of the highest and lowest rainfall as well as highest and lowest NRCS intensity values were counted. For pixels 1 to 8 (Area 1), Fig. 5.9 summarizes the situation.

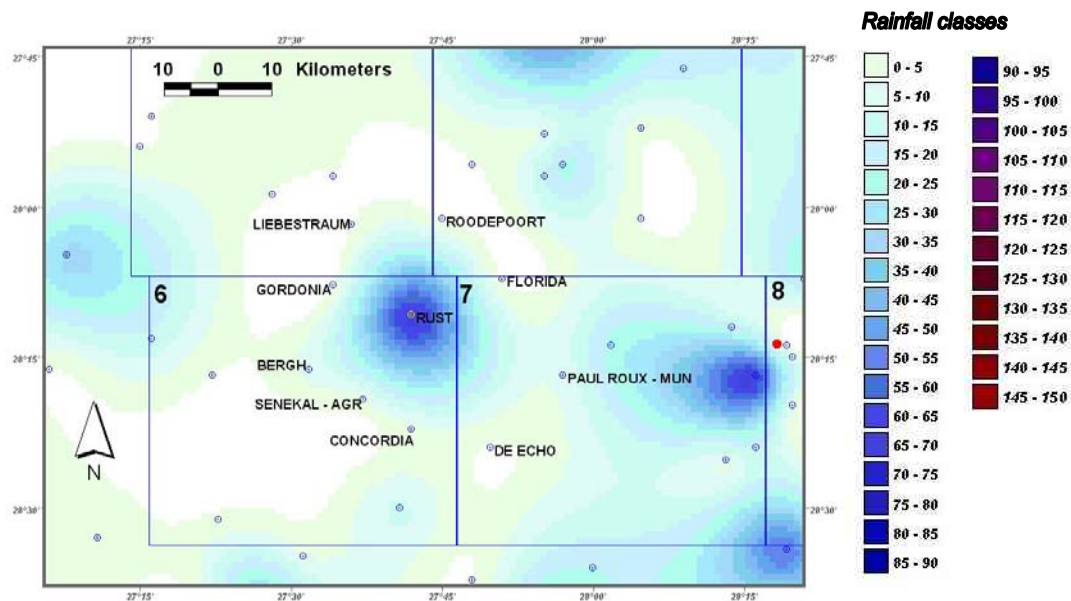


Figure 5.8: Rainfall at meteorological station Rust and its neighbours within various WSC database pixels (rainfall in mm; sources: ESA, 2001; South African Weather Service, 2003; data manipulation: ArcView GIS software).

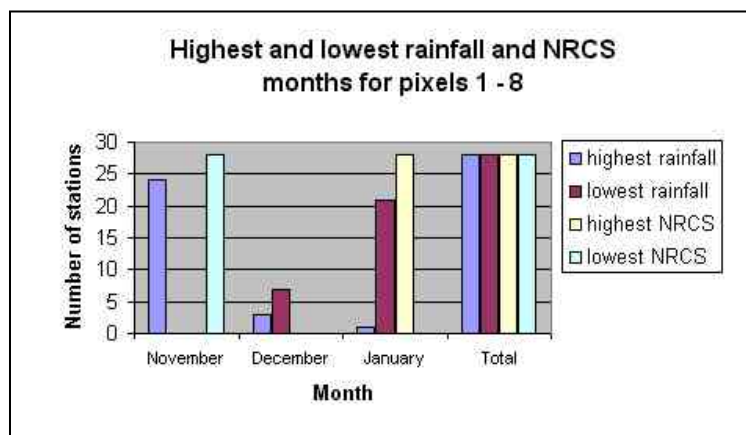


Figure 5.9: Months of highest and lowest rainfall and NRCS (pixels 1 to 8; sources: ESA, 2001; South African Weather Service, 2003; data manipulation: MS Excel).

It is clear that the month with the highest rainfall for most meteorological stations occurs in November 1998. The month with the lowest NRCS intensity values also occurs in November, applicable to all meteorological stations. For the majority of meteorological stations, the month with the lowest rainfall occurs in January 1999, while the month with the highest NRCS intensity values occurs in the same month for all meteorological stations. This shows a negative correlation between monthly rainfall and monthly NRCS intensity values for this area in this time.

In pixels 9 to 17 (Area 2), the trend is different (Fig. 5.10). The month with the highest NRCS intensity values is the same month for the most meteorological stations' month with the lowest rainfall: December. The month with the highest rainfall and the month with

the lowest NRCS intensity values is the same as for pixels Area 1: November. The month January displays more confusion where the lowest NRCS intensity values joins with some incidents of the highest and lowest rainfall. No positive correlation was discovered between rainfall figures and NRCS intensity values. It rather seems to be a negative correlation, however not as strong as the one in Area 1.

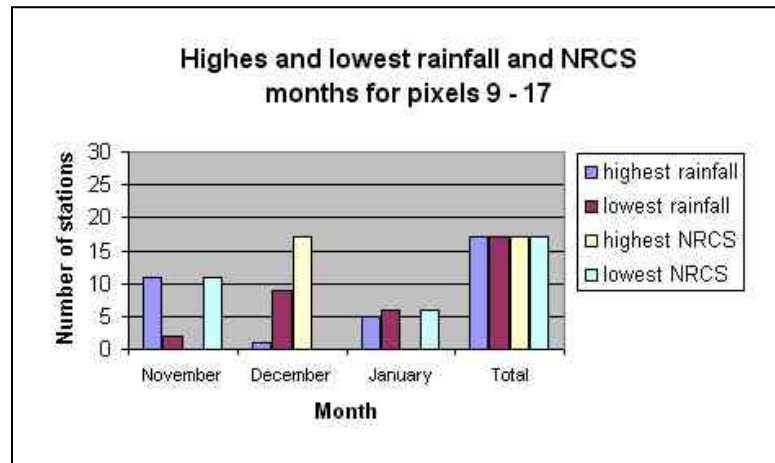


Figure 5.10: Months of highest and lowest rainfall and NRCS (pixels 9 to 17; sources: ESA, 2001; South African Weather Service, 2003; data manipulation: MS Excel).

5.2.5 Modelling NRCS intensity values with daily rainfall data

A model is used to get more insight into the relation between daily rainfall and NRCS intensity values. In short: weights are assigned to the number, length and intensity of rainfall events per month per meteorological station. The results of these weighted data are then used to calculate the spread of rainfall days through the month. This is multiplied with the real monthly rainfall to come up with a value that resemble expected NRCS intensity value behaviour in that month, but only based on rainfall data.

The definition of a rainfall event can be described by the example in Fig. 5.11. For example, one rainfall event occurs from 17 to 20 November for a period of four days. A day can be classified as a rainfall day when there is a recording of rainfall in mm above 0 mm on that day. The example of the meteorological station at Petra, pixel 8, will be used to explain the model.

At first the number of rainfall events is counted per month. In the case of the meteorological station at Petra in November – the number of rainfall events is 7. Then the number of n -day long rainfall events is counted (where n is the length of each rainfall event in days). For the meteorological station at Petra it comes down to this: 2 rainfall events of one day long, 3 rainfall events of 2 days long, 1 rainfall event of 3 days long and 1 rainfall event of 4 days long. The total number of rainfall days is 15.

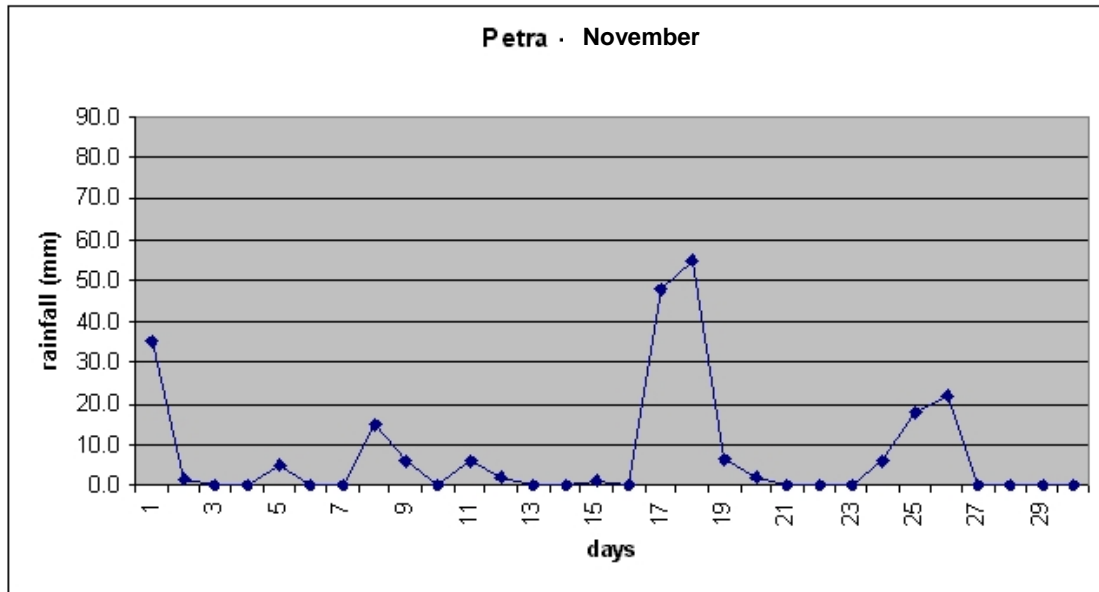


Figure 5.11: Rainfall events for meteorological station at Petra in November 1998 (source: South African Weather Service, 2003; data manipulation: MS Excel).

The following formula can be used to calculate the total number of rainfall days per month from the rainfall events, or one can most simply count them from the graph:

$$x = (1 \times a) + (2 \times b) + (3 \times c) + (4 \times d) + (5 \times e) + \dots + (31 \times x) \quad \mathbf{5.1}$$

- where:
- x = number of rainfall days
 - a = number of 1 day-long rainfall events
 - b = number of 2 day-long rainfall events
 - c = number of 3 day-long rainfall events
 - d = number of 4 day-long rainfall events
 - e = number of 5 day-long rainfall events

There are no rainfall events longer than 5 days at any meteorological station. The assumption is made that longer rainfall events can be associated with more rainfall and cloudiness, less evaporation, higher soil moisture levels for prolonged periods of time and thus higher NRCS intensity values. Weights are assigned according to the length of a rainfall event to calculate the weighted number of rainfall days:

$$vx = (1 \times a \times 1) + (2 \times b \times 1.2) + (3 \times c \times 1.4) + (4 \times d \times 1.6) + (5 \times e \times 1.8) \quad \mathbf{5.2}$$

- where: vx = weighted number of rainfall days based on rainfall events

Rainfall days are classified into three classes according to precipitation in mm: 1-30 mm; 30-60 mm; 60-90 mm (the lower class boundary is inclusive while the upper boundary is exclusive). They are counted to come to the total number of rainfall days:

$$x = f + g + h \quad \mathbf{5.3}$$

where: f = number of rainfall days in class 1-30 mm
 g = number of rainfall days in class 30-60 mm
 h = number of rainfall days in class 60-90 mm

There are no days with more than 90 mm of precipitation at any meteorological station. Another assumption is made that the more precipitation, the higher the soil moisture will be and consequently the higher the NRCS intensity value will be. Weights are assigned according to the precipitation class to calculate the weighted number of rainfall days.

$$wx = (f \times 1) + (g \times 1.2) + (h \times 1.4) \quad \mathbf{5.4}$$

where: wx = weighted number of rainfall days based on precipitation

The average of the two sorts of weighted rainfall days (vx and wx) is calculated, again with a weight introduced to get to the final number of weighted rainfall days. It is assumed that the length of rainfall events, even with relatively low precipitation, might have a larger influence on the increase of soil moisture (and thus NRCS intensity values) than high single day precipitation rates:

$$Wx = (vx \times 1.2) + wx / 2 \quad \mathbf{5.5}$$

where: Wx = final number of weighted rainfall days

This (Wx) is not the real number of rainfall days, but a weighted value that takes into account the length of rainfall events as well as the amount of precipitation. For the meteorological station at Petra with a normal number of rainfall days of 15, the weighted number of rainfall days is 19,7.

The 'normal spread' of the rainfall days is calculated per month as a percentage of days that it rained per month:

$$s = (x / 30) \times 100 \quad \mathbf{5.6}$$

where: s = normal spread of rainfall days

For the meteorological station at Petra, the normal spread is calculated as 50% (15 days of November with 30 days). This percentage does not take into account the length and number of rainfall events as well as precipitation levels. The weighted spread is calculated by using the final number of weighted rainfall days:

$$ws = (W_x / 30) \times 100 \quad \mathbf{5.7}$$

where: ws = weighted spread of rainfall days

For the meteorological station at Petra this resulted in a weighted spread of 65.6% (19,7 weighted days in November with 30 days). Now the weighted spread is multiplied with the total rainfall (in mm) in the same month to calculate the weighted NRCS intensity value.

$$pN = ws \times r \quad \mathbf{5.8}$$

where: pN = weighted NRCS intensity value (not scaled to normal backscatter range)

r = total rainfall per month

According to the model the resulting value will be very high when the length and number of rainfall events are high and when precipitation rates per rainfall day is high. When the opposite is true the resulting value is expected to be much lower. This value (weighted NRCS intensity value) is a model value for the behaviour of NRCS intensity values when only rainfall is taken into account. For the meteorological station at Petra with a total precipitation of 229 mm in November, this value is calculated as 15022,4. In the end this value is not interesting in itself, but only when compared to monthly rainfall and NRCS intensity values and their behaviour over the three months. This weighted NRCS intensity value is divided with 100 to make it smaller and graphically comparable to the total rainfall per month. The real monthly NRCS intensity values are in their turn multiplied by 100 to make them graphically comparable to the monthly rainfall and weighted NRCS intensity values. Fig. 5.12 shows the lines of the total monthly rainfall, weighted NRCS intensity values as well as real NRCS intensity values.

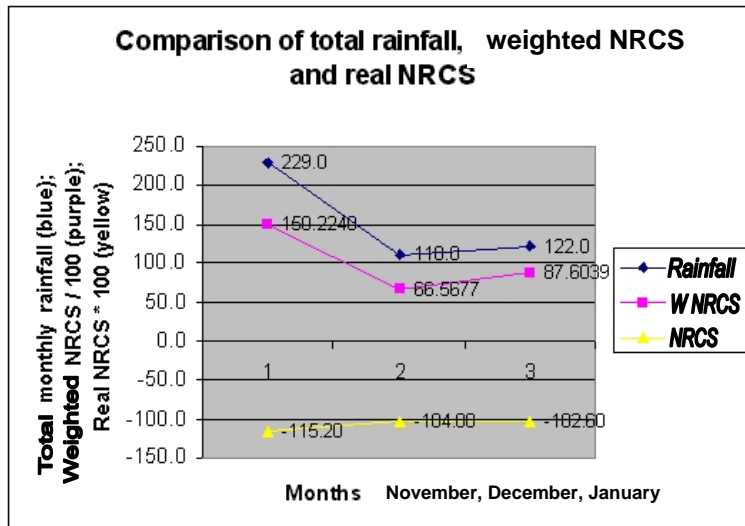


Figure 5.12: Comparison of total rainfall, weighted NRCS intensity values and real NRCS intensity values, meteorological station at Petra (sources: ESA, 2001; South African Weather Service, 2003; data manipulation: MS Excel).

To compare Fig. 5.12 with the actual monthly rainfall situation at the meteorological station Petra, refer to appendix 9 where the daily rainfall patterns per month are displayed.

It is clear that although the weighted NRCS line follows the total rainfall line in terms of pattern, the relative weighted NRCS intensity values increases from November to January in terms of its distance from the rainfall line. This is due to longer rainfall events that occur in December and January when compared to November. It is however also clear that the weighted NRCS line does not resemble the pattern of the real NRCS line at all. This is due to the fact that only rainfall data have been used in this model.

This model was applied to all the selected meteorological stations in all the selected pixels (Fig. 5.4). In all of them, the line of weighted NRCS intensity values show a much stronger relation with the rainfall line and very little resemblance to the real NRCS line. In the few cases where the weighted NRCS line resembles the form of the real NRCS line for all three months, it is not very accurate. It is however interesting to note that these cases occur mostly in the area of pixels 9 to 17 (Area 2). These are the meteorological stations at Dankbaar (pixel 10), Smithfield municipality (pixel 15) and Tweefontein (pixel 16). In pixels 1 to 8 (Area 1) there is no resemblance between the weighted and real NRCS lines. This suggests that the NRCS intensity values in the southern areas in the Free State react more to rainfall than to the presence and growth of vegetation. This is not the case in the north-eastern parts where agricultural vegetation is much more common at these times of the year.

6. Discussion

The results (including those of the model) suggest that there are more factors that influence NRCS intensity values' behaviour than rainfall alone. It is assumed that in pixels 1 to 8 (Area 1) vegetation has a strong influence on the increase of monthly NRCS intensity values. Although the rainfall figures decrease from December '98 to January '99, vegetation growth increases. Radar backscatter intensity increases when the vegetation canopy is dense and healthy. This is mainly due to the moisture in the leaves. Pixels 1 to 8 (Area 1) cover an area where agriculture is the main land use (Appendix 4). Unfortunately no field information is available for direct verification.

It is not clear what the situation is in the area of pixels 9 to 17 (Area 2). The general trend is also that an increase in rainfall figures is associated with a decrease in NRCS intensity values. The assumption is made that due to the arid climate of this area, increased rainfall will not affect NRCS intensity values strongly. Due to its main known land cover (grassland and shrubland, Appendix 4), no agricultural vegetation occurs in these areas that could increase radar backscatter intensities. After a rainfall event (they are usually quite short in this area), evaporation may have a strong influence (when prolonged periods of cloudiness do not exist) on the loss of soil moisture. In a seasonal study conducted by Scipal et al. (2002) in a steppe environment in Mali, NRCS intensity values were not affected by separate rainfall events due to high evaporation rates at the beginning of the rainy season. Only after prolonged rainfall events in the rainy season did NRCS intensity values increase until the height of the rainy season. Although this was not a seasonal study, the south-western part of the Free State is a similar landscape when compared to the steppes in Mali. It is a recommendation to study the seasonal variations of NRCS intensity values and rainfall data in the Free State. It is expected that the south-western parts of the province will show similar seasonal patterns as in Mali, different from areas with more vegetation.

Slightly more evidence was found for a small positive correlation between rainfall data and NRCS intensity values in this arid area in specific instances (Chapter 5.2.2); this can be linked to the results of Woodhouse and Hoekman (n.d.). They found a strong correlation between monthly rainfall data and monthly NRCS intensity values in the Sahel. The Sahel is a dry and arid area while the southern parts of the Free State (Area 2) are also arid but perhaps not as arid as the Sahel. This may however explain why there is more evidence of a positive correlation between rainfall and NRCS intensity values in pixels 9 to 17 (Area 2) than in pixels 1 to 8 (Area 1). Wagner et al. (1996) concluded that soil moisture information can be retrieved from NRCS intensity values in areas where vegetation is moderate. The conclusion here is that where vegetation is relatively sparse, the NRCS intensity values will be less affected by vegetation and more by (soil) moisture, amongst others related to preceding rainfall. The conclusion is that there are stronger correlations between monthly rainfall and

NRCS intensity values in arid areas than in areas that are less arid and more vegetation rich. This makes sense as vegetation can increase NRCS intensity values significantly even if rainfall or other soil moistening factors are absent. If no vegetation exists, or when vegetation is a minor land cover type, NRCS intensity values can only increase when bare soil areas are moistened by rainfall or other factors like dew or fog.

It was interesting to discover that the 3-month averages for rainfall figures as well as NRCS intensity values show a strong positive correlation. The conclusion is that the correlation is more positive over longer periods of time, also according to Frison (1998) and Jarlan (2002). From this follows that the more arid an area, the higher the correlation will be between rainfall figures and backscatter intensity data over shorter periods of time. The correlation between rainfall figures and backscatter intensity data for vegetation rich areas will show positive correlations only over longer periods of time.

Because of a lack of field data and more accurate meteorological data per station (cloudiness, temperature, sunshine hours), the model (Chapter 5.2.5) was only based on the rainfall data that was available. This is a rather important shortcoming of the model. Some other generalisations are present as well. One example is the classification used to classify the meteorological stations into classes of precipitation amount (formula 5.3). It would have been more precise if more classes were used. Another shortcoming of the model is that it does not predict daily NRCS intensity values. It uses daily rainfall data to calculate a value on a monthly basis. A model predicting daily NRCS intensity values from meteorological data will only be good if complete daily meteorological and field data is available and incorporated into the model.

Full temporal resolution scatterometer data is however available from Cersat (http://www.ifremer.fr/cersat/DATA/E_DATA.htm). The maximum temporal resolution is then about 4 days. Full temporal resolution data was extracted from the website of Cersat, but unfortunately no time and expertise existed to convert this data into a usable format. One needs to write a new software application to work with the data.

This may in fact be an excellent opportunity for a following research project - to study the relationships between full resolution NRCS intensity data and daily meteorological data (including rainfall, cloudiness, temperature and sunshine ours). Another suggestion for a following research project is to monitor the behaviour of rainfall and NRCS intensity data for one complete year. Together with complete meteorological data and field data, this may enhance the understanding of seasonal variation in NRCS intensity values.

The use of a radar sensor with a higher spatial resolution (like Radarsat) may prove to be useful. A cost factor will then be introduced as Radarsat data is not available free of charge. This is however not the case with data from the ERS scatterometer; it can be obtained free of charge. The ERS scatterometer is furthermore better suited to study regional and

global processes but not local processes (Wagner et al., 1996). Although the Free State is quite large, the variations in daily rainfall cannot be studied on a regional basis but rather on a local one. Radarsat data may then be more useful.

Various recent studies focus on the use of scatterometer data for estimating soil moisture as well as using the soil moisture data operationally. Scipal & Wagner (2004) as well as Bartalis et al. (2005) explores the possibilities of creating global soil moisture databases that can be used climatological and meteorological applications. Scipal et al. (2005) and Parajka et al. (2006) shows that coarse resolution scatterometer data can provide hydrologic relevant information to be used for soil moisture and runoff related river basin scale (regional) studies when using various hydrological models. Hasenauer et al. (2006) explores the possibilities of a near-real time soil moisture database based on ERS scatterometer data for hydrology and water management, numerical weather prediction as well as land surface applications. The application of ERS scatterometer data is thus operational in terms of soil moisture estimation. This goes beyond the comparison of the scatterometer data with rainfall data.

It is unfortunate that it is so difficult to integrate the WSC-data with other data due to format and software restrictions. Fully interoperable data would have made a lot of data processing much easier, faster and more worthwhile as more interesting relations in the data could have been explored. The WSC database may have to undergo some upgrades in terms of the interoperability standards that are developed by international institutions like ISO TC/211 (<http://www.isotc21.org/>) and GSDI (Global Spatial Data Infrastructure, <http://www.gsdi.org/>).

7. Conclusion

The relation between rainfall data and the data of the WSC database was investigated in this study. Daily rainfall data was available while only monthly scatterometer data was available. A positive correlation was found between the 3-monthly average of rainfall and NRCS intensity values suggesting a higher correlation between rainfall and NRCS intensity values over a longer term. No specific positive correlation was found on a monthly basis for this area and time of the year; rather a negative correlation was dominant at the majority of meteorological stations. There was however some evidence that positive correlations exist in the more arid parts in the south of the Free State province. This is supported by literature where positive correlations are found between monthly rainfall data and monthly NRCS intensity values in arid areas. It is assumed that the growth of plants in the northern parts of the province results in an increase of NRCS intensity values, even if rainfall figures decrease. Consequently these NRCS intensity values do not show a positive correlation to rainfall data.

Daily rainfall data was used in a model to see whether it could be used to detect a relation between daily rainfall and monthly NRCS intensity values. No specific relation was found. The model is however based only on daily rainfall data and not on other meteorological or field data and thus has definite shortcomings. The spatial variation of daily rainfall can be very high over an area that has the size of a WSC database pixel (50 * 50 km). It is difficult to capture this variation with one NRCS intensity value per month. Unfortunately the available scatterometer data of higher temporal resolution could not be used due to conversion troubles and a shortage of time. This data would enable one to study the relation between rainfall and radar data on at least a weekly basis.

Remote Sensing is a very useful tool for agricultural management. It is however important to know what the suitable spatial and temporal resolution of the remotely sensed data must be in order to study phenomena in, on and above the earth. Non-applicable resolutions that are chosen to study certain phenomena may lead to incomplete or false results and consequently to poor decision making in agriculture. In the case of this research project a Remote Sensing tool (WSC database) with a spatial resolution of 50 km and a temporal resolution of 1 month is not applicable to be used in comparison with daily rainfall data. A higher spatial and temporal resolution is needed for this to get clear, reliable and accurate results.

REFERENCES

- Bartalis, Z., Scipal, K. & Wagner, W. 2005. Soil moisture products from C-band scatterometers: From ERS-1/2 to METOP. *ENVISAT & ERS Symposium*. Salzburg, Austria, 6-10 September 2004. ESA SP-572, Pages 1417-1423.
- Boogaard, H.L., van Diepen, C.A., & Savin, I. 2000. *Monitoring drought affected crop yields based on ERS-scatterometer data; Exploration of possibilities to integrate ERS scatterometer derived soil moisture into the CGMS crop model for a Russian-Ukrainian study area*. Wageningen: Alterra Green World Research. Rapport 009.
- Cersat. n.d. *Data distributed by CERSAT*. Cersat: Plouzané.
http://www.ifremer.fr/cersat/DATA/E_DATA.htm
- Digital Chart of the World. 1997. *Administrative boundaries of South Africa*.
- ENPAT. 2000a. *Environmental Potential Atlas for the Free State. Mean Annual Precipitation*. Pretoria: Department of Environmental Affairs and Tourism.
- ENPAT. 2000b. *Environmental Potential Atlas for the Free State. Land Cover*. Pretoria: Department of Environmental Affairs and Tourism.
- ESA (European Space Agency). 2001. *Wind Scatterometer database of the world (August 1991 to August 1999)*. Noordwijk: ESA.
- Frison, P.L., Mougín, E., & Hiernaux, P. 1998. Observations and Interpretation of Seasonal ERS-1 Wind Scatterometer Data over Northern Sahel (Mali). *Remote Sensing of Environment*. Vol. 63. 233 – 242.
- Global Spatial Data Infrastructure. 2003. *GSDI homepage*. Global Spatial Data Infrastructure
<http://www.gsdi.org/>
- Hasenauer, S., Wagner, W., Scipal, K., Naeimi, V. & Bartalis, Z. 2006. Implementation of near real-time soil moisture products in the SAF network based on MetOp ASCAT data. *EUMETSAT Meteorological Satellite Conference*. Helsinki, 12–16 June 2006.
- Hoekman, D.H. & van Oevelen, P.J. 2002. *Course: Remote Sensing Physics and Radar*. Wageningen: Wageningen University and Research Centre.
- Institute for Applied Remote Sensing. 2000. *Eight Years of ERS Scatterometer Data over Land on a Single CD-ROM*. The Institute for Applied Remote Sensing: Freiburg.

<http://www.ifars.de/> (click on Scatdb)

International Organization for Standardization. 2003. *ISO/TC 211. Geographic information/Geomatics*.
ISO/TC 211: Kartverksveien.

<http://www.isotc211.org/>

Jarlan, L., Mougin, E., Frison, P.L., Mazzega, P. & Hiernaux, P. 2002. Analysis of ERS wind scatterometer time series over Sahel (Mali). *Remote Sensing of Environment*. Vol. 81. 404–415.

Johannessen, O.M., Sandven, S., Jenkins, A.D., Durand, D., Pettersson, L.H., Espedal, H., Evensen, G. & Hamre, T. 2000. Satellite earth observation in operational oceanography. *Coastal Engineering* Vol. 41. 155 – 176.

Lillesand, T.M. & Kiefer, R.W. 2000. *Remote Sensing and Image Interpretation*. 4th edition. New York: John Wiley & Sons.

Parajka, J., Naeimi, V., Blöschl, G., Wagner, W., Merz, R. & Scipal, K. 2006. Assimilating scatterometer soil moisture data into conceptual hydrologic models at the regional scale. *Hydrology and Earth System Sciences*. Vol. 10. 353-368.

Scipal, K., Scheffler, C. & Wagner, W. 2005. Soil moisture-runoff relation at the catchment scale as observed with coarse resolution microwave remote sensing. *Hydrology and Earth System Sciences*. Vol. 9. Issue 3. 173-183.

Scipal, K., Wagner, W., Kidd, R. & Ringelmann, N. 2002. Comparison of Ku- and C- Band Backscatter Time Series over Land. *IEEE*.

http://www.ipf.tuwien.ac.at/publications/ks_ww_toronto02/TH04_582.pdf

Scipal, K. & Wagner, W. 2004. Global soil moisture data and its potential for climatological and meteorological applications. *The 2004 EUMETSAT Meteorological Satellite Conference, Prague*. 31 May - 4 June 2004.

South African Weather Service. 2003. *Daily rainfall data for the Free State province in South Africa*. South African Weather Service: Pretoria.

<http://www.weathersa.co.za/>

Wagner, W., Borgeaud, M. & Noll, J. 1996. *Soil moisture mapping with the ERS Scatterometer*. ESA.

<http://esapub.esrin.esa.it/eoq/eoq54/wagne54.htm>

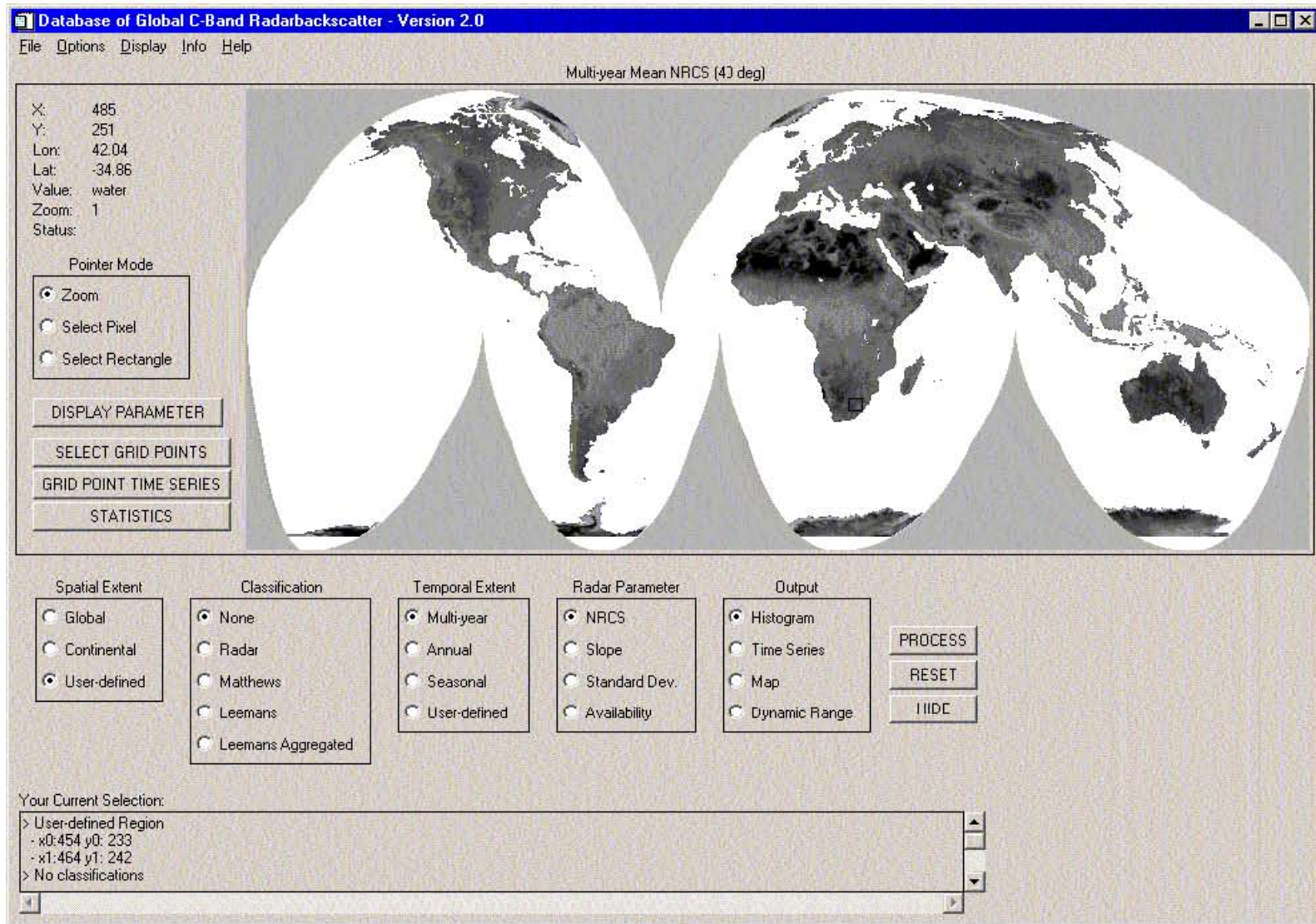
Wagner, W. 1998. *Soil Moisture Retrieval from ERS Scatterometer Data*. Unpublished PhD research

report. Vienna: Vienna University of technology.

Wismann, V. 1999. A database of global C-band NRCS derived from ERS scatterometer data. *IEEE Geoscience and Remote Sensing Newsletter*. Vol. 106. 7-9.

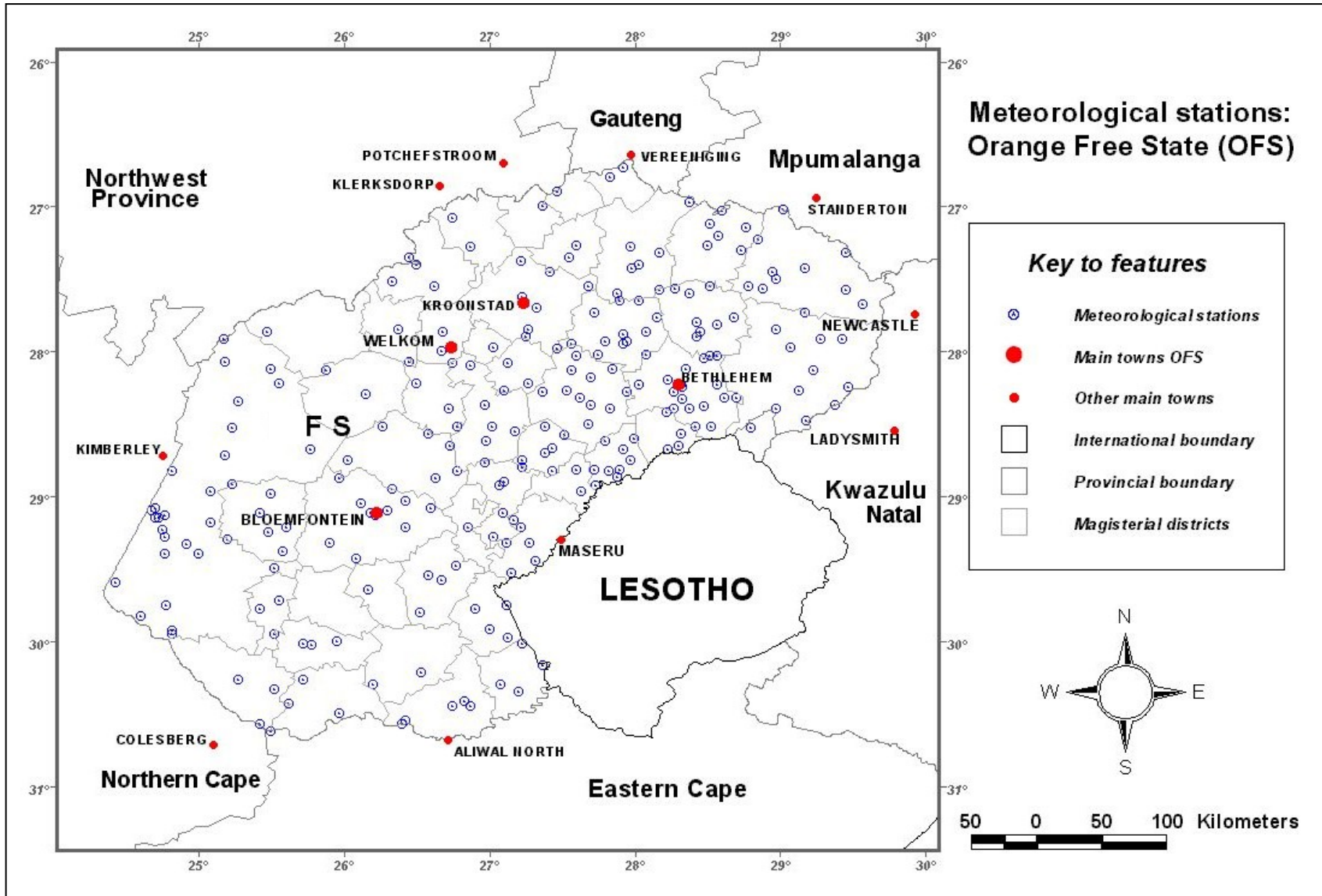
Wismann, V. & Lin, C.C. 2003. *Personal conversation via e-mail*.

Woodhouse, I. & Hoekman, D. n.d. *Land Surface Parameter Retrieval -Geophysical Inversion Using a Mixed-Target Model*. Freiburg: IFARS. <http://www.ifars.de/>

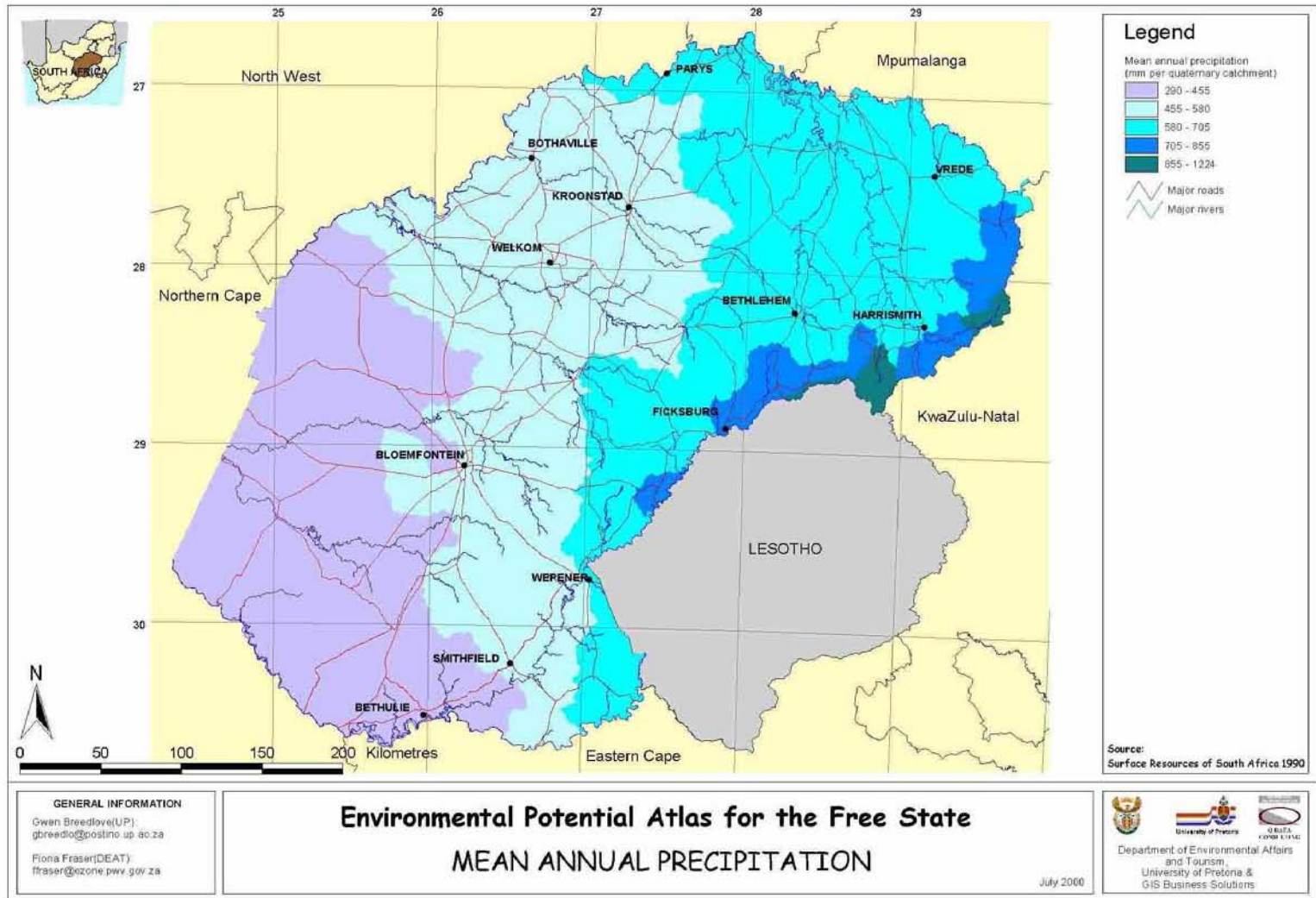


APPENDIX 1: Interface designed to work with scatterometer data (source: ESA, 2001; data manipulation: WSC database application).

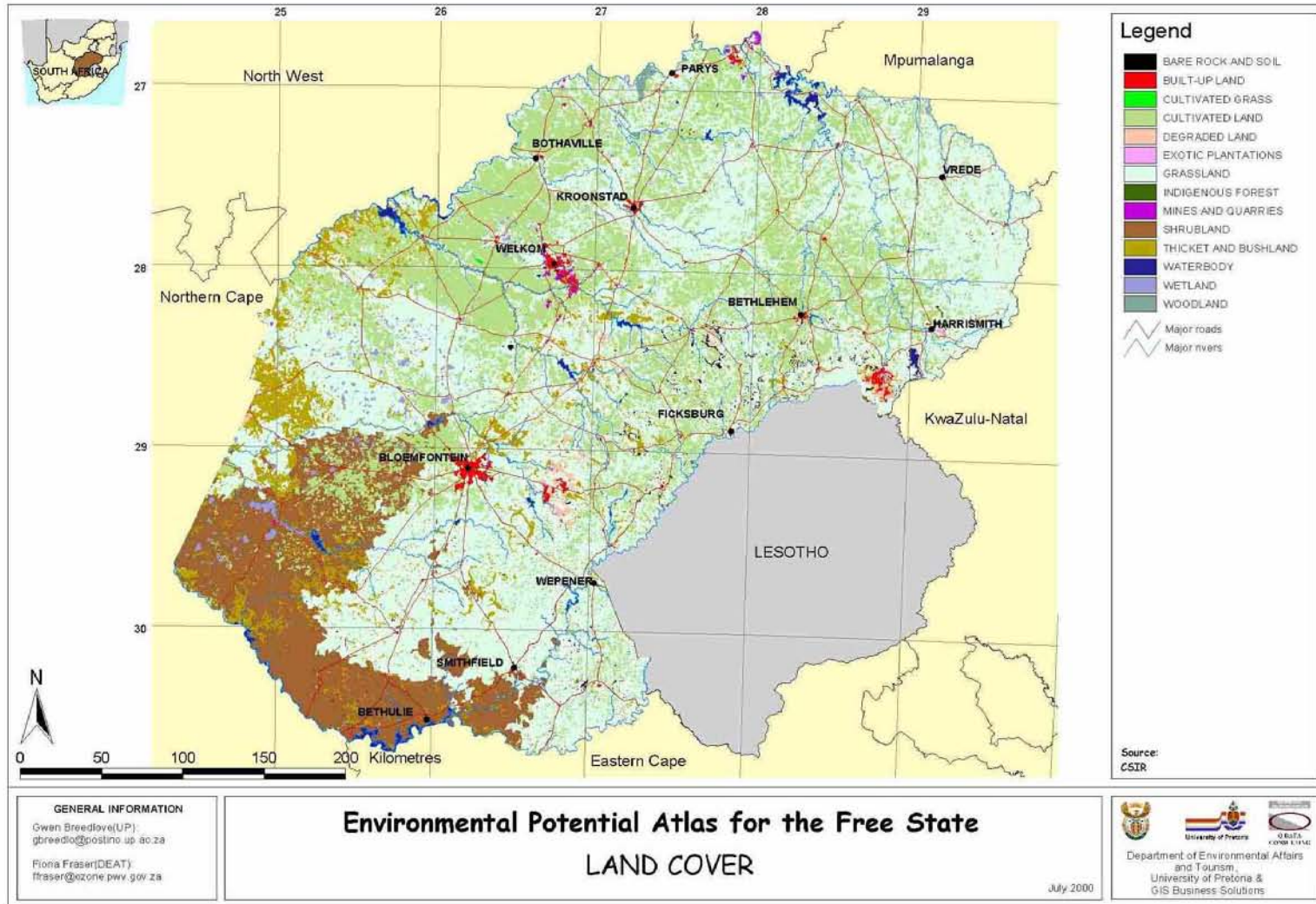
LIST OF APPENDICES



APPENDIX 2: Meteorological stations in the Free State (source: South African Weather Service, 2003; data manipulation: ArcView GIS software).

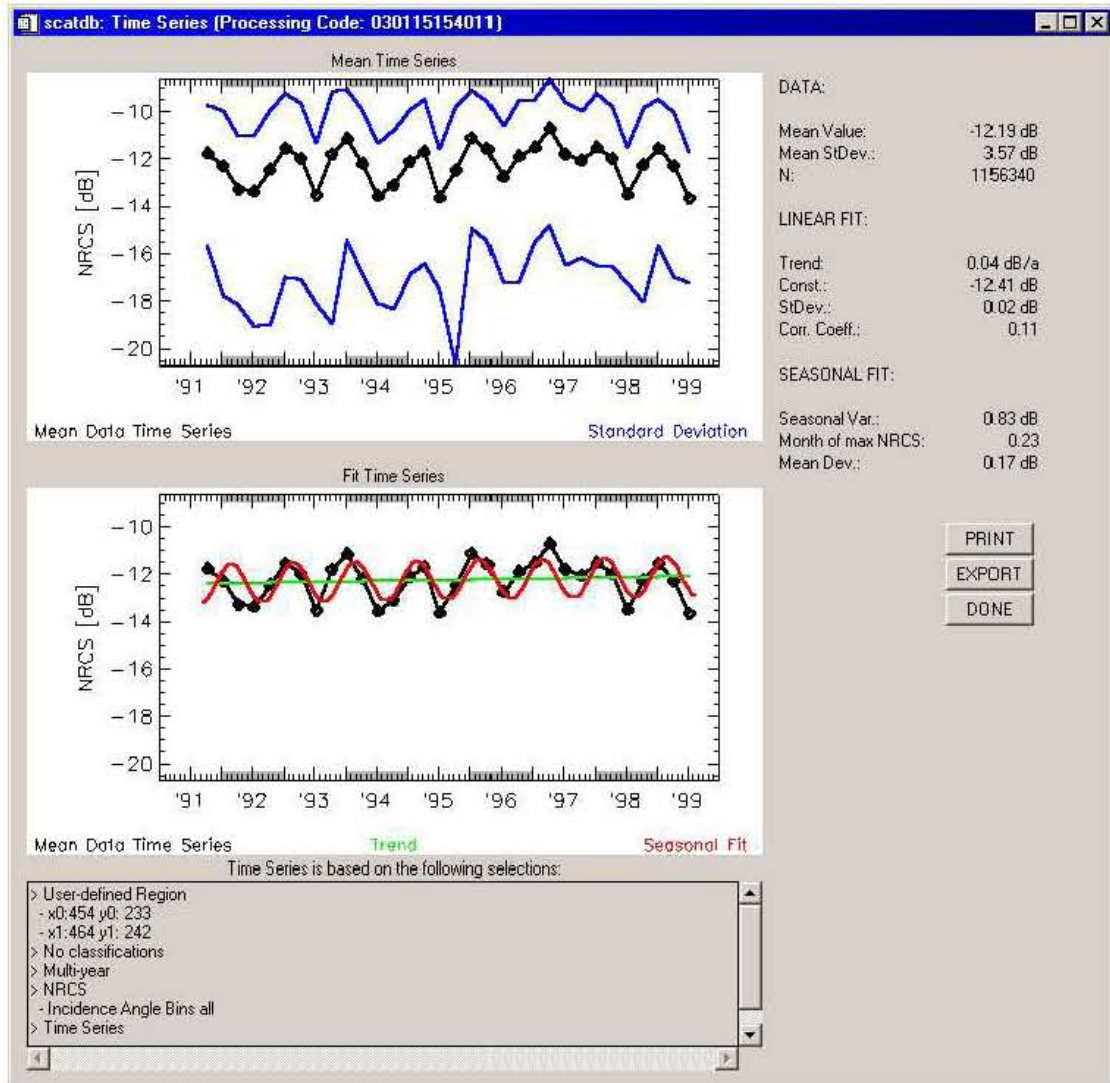


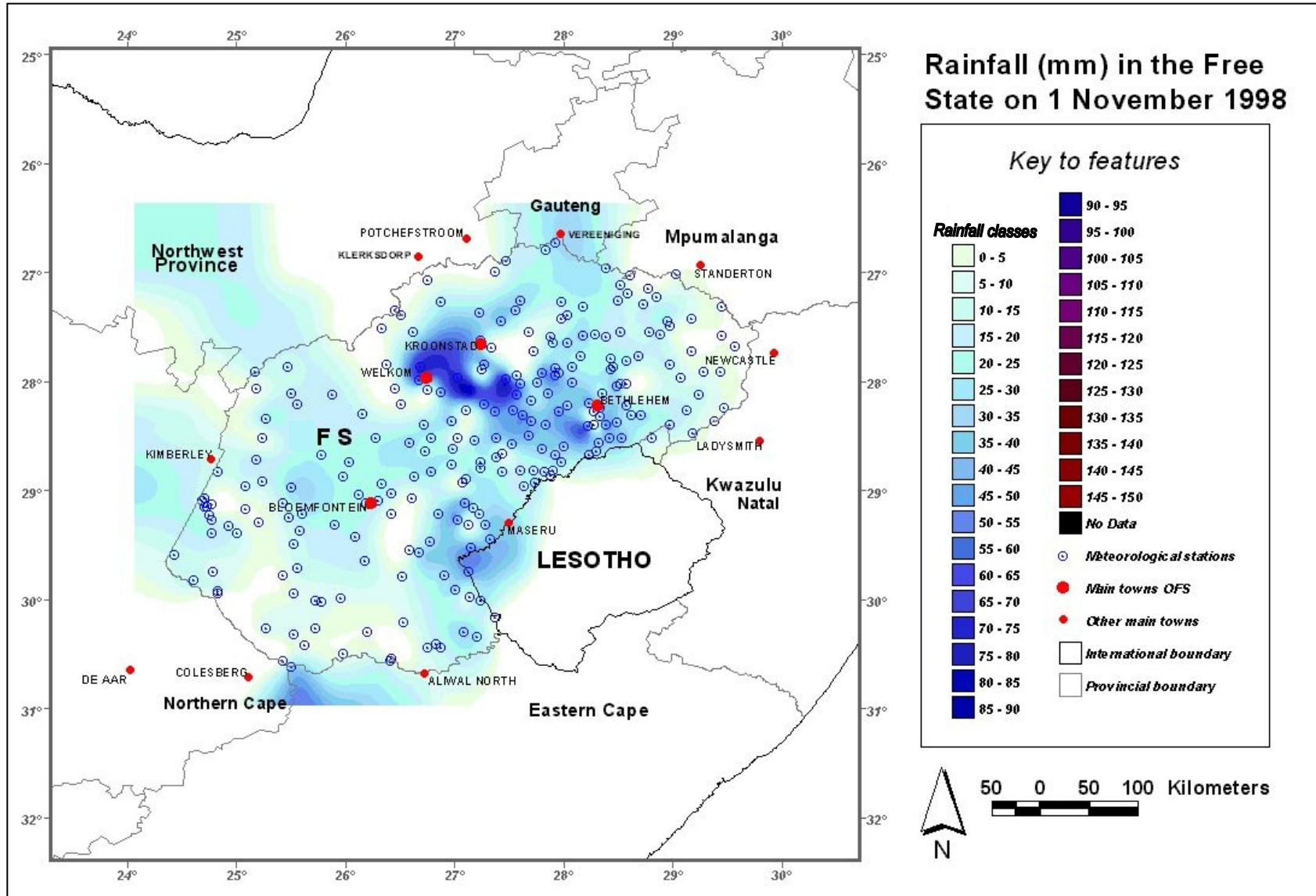
APPENDIX 3: Annual precipitation rates for the Free State (source: ENPAT, 2000a).



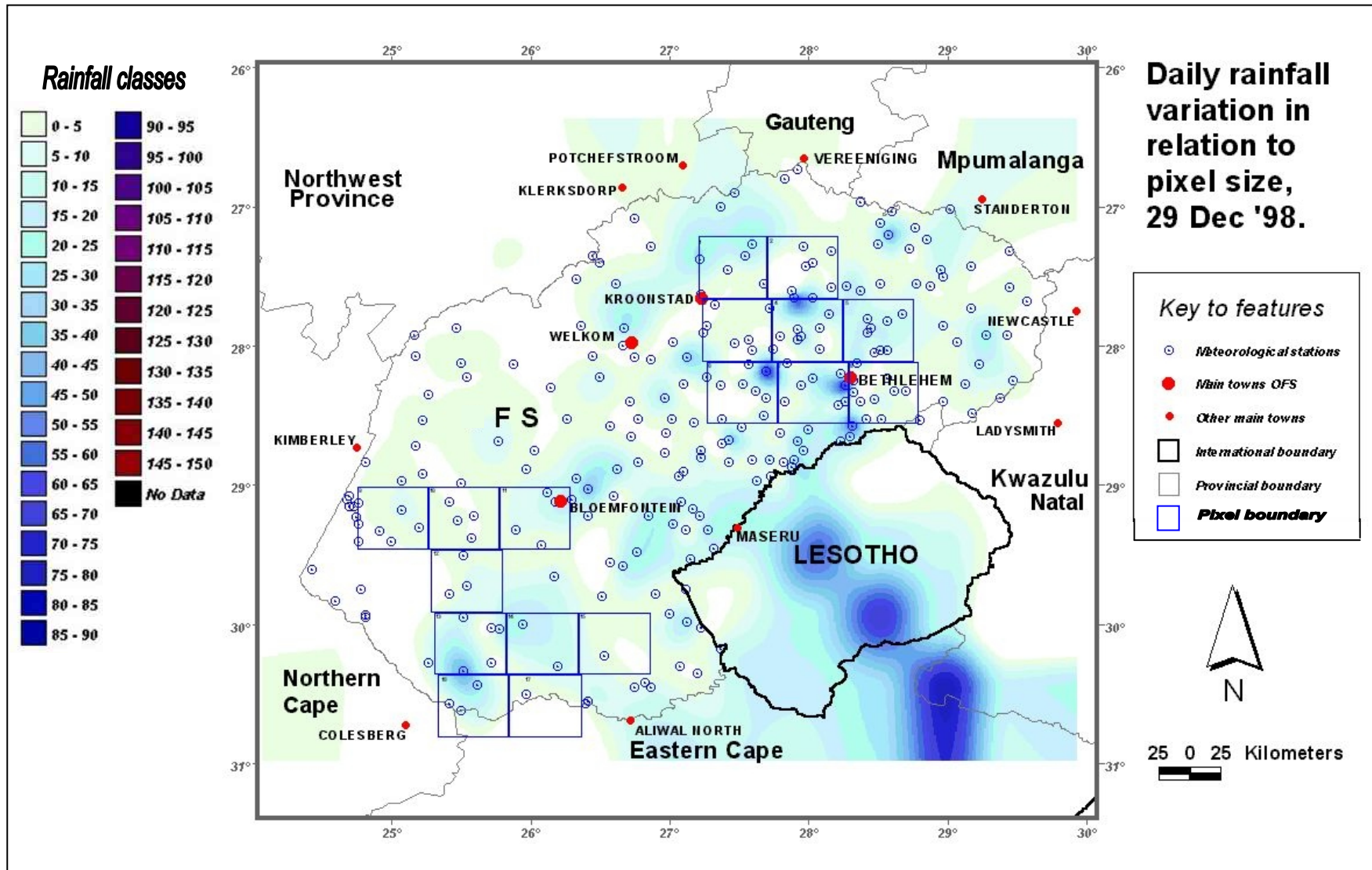
APPENDIX 4: Land cover types in the Free State (source: ENPAT, 2000b).

APPENDIX 5: Time series of NRCS intensity values in box around the Free State province (source: ESA, 2001; data manipulation: WSC database application).



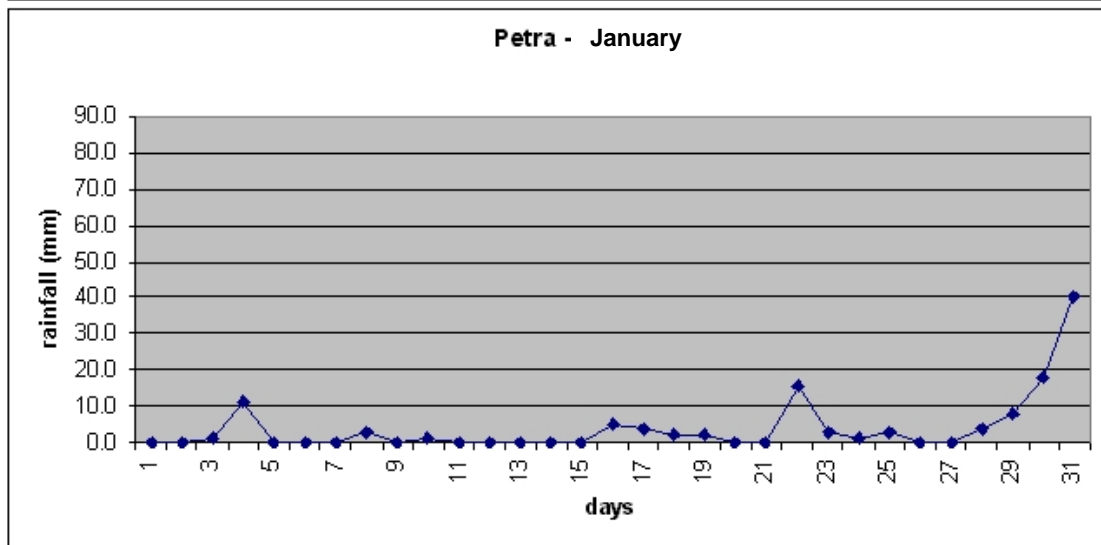
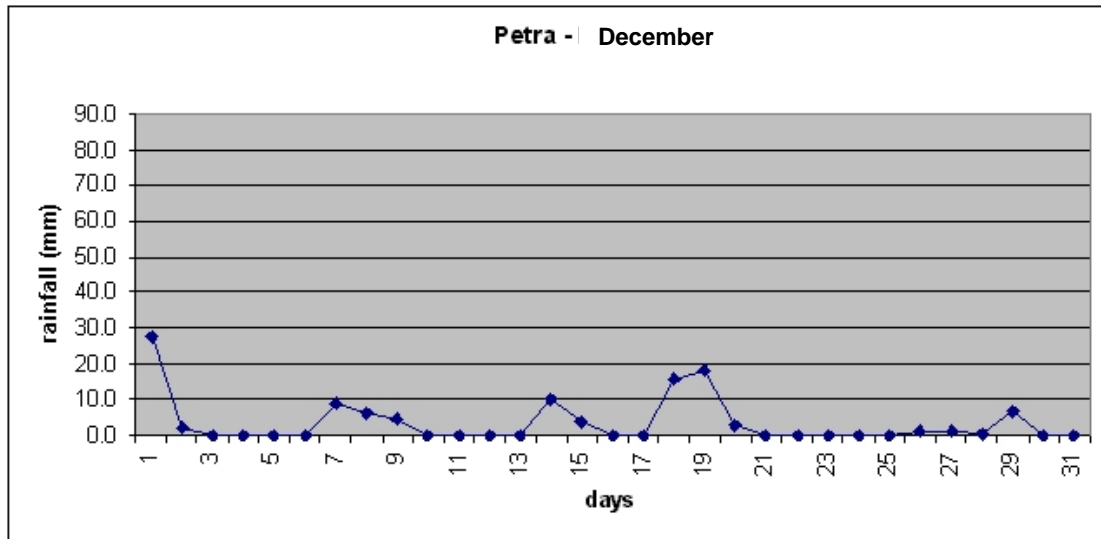
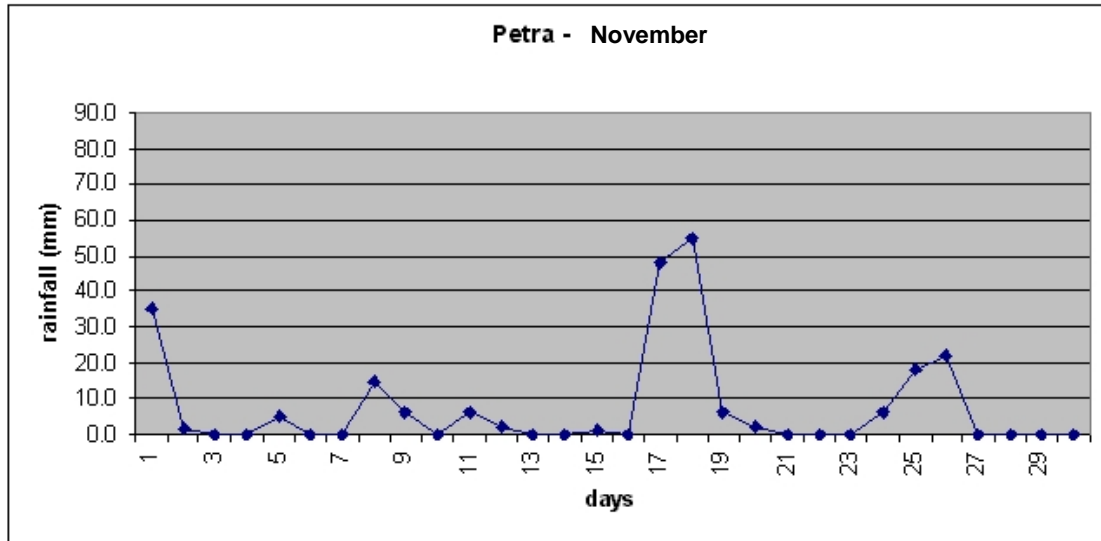


APPENDIX 6: Rainfall map of the Free State on 1 November 1998 (source: South African Weather Service, 2003; data manipulation: ArcView GIS software).



APPENDIX 8: Daily rainfall variations in relation to pixel size (source: South African Weather Service, 2003; data manipulation: ArcView GIS software).

APPENDIX 9: Daily rainfall patterns per month for meteorological station at Petra (source: South African Weather Service, 2003; data manipulation: MS Excel).

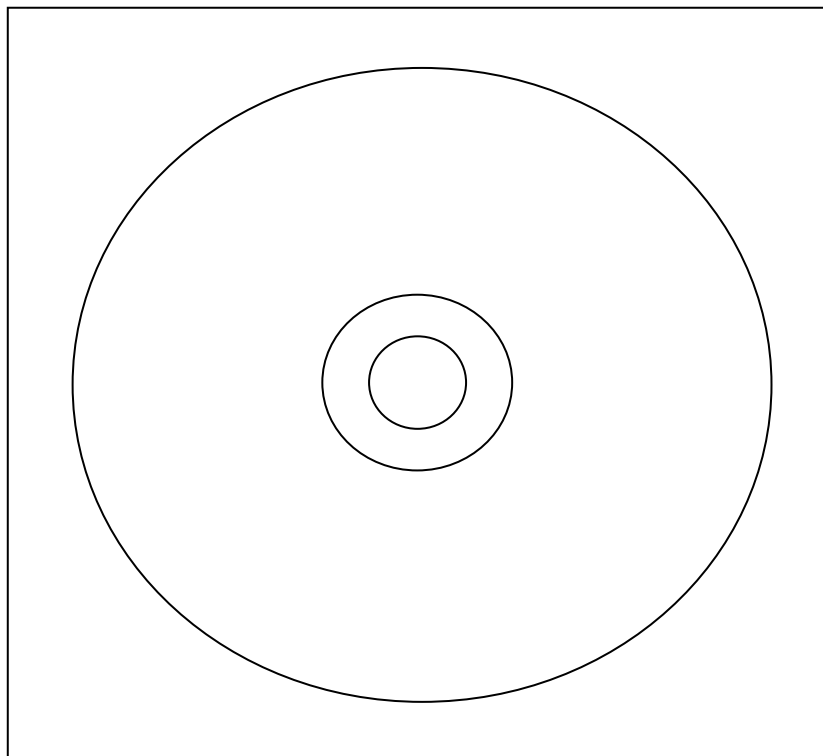
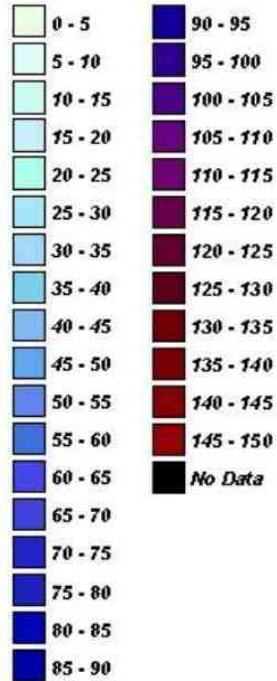


POWERPOINT TIME SEQUENCES

(Source: South African Weather Service, 2003; data manipulation: MS PowerPoint)

In this additional CD-ROM there are three PowerPoint files. Each file contains an animation of daily rainfall in the Free State province per month. These files and their information are described in Chapter 5.1.2. The source data comes from the South African Weather Service. The data interpolation was prepared with ArcView GIS software. The files can be viewed with MS PowerPoint. The rainfall data classes are shown below in mm per day.

Rainfall classes:



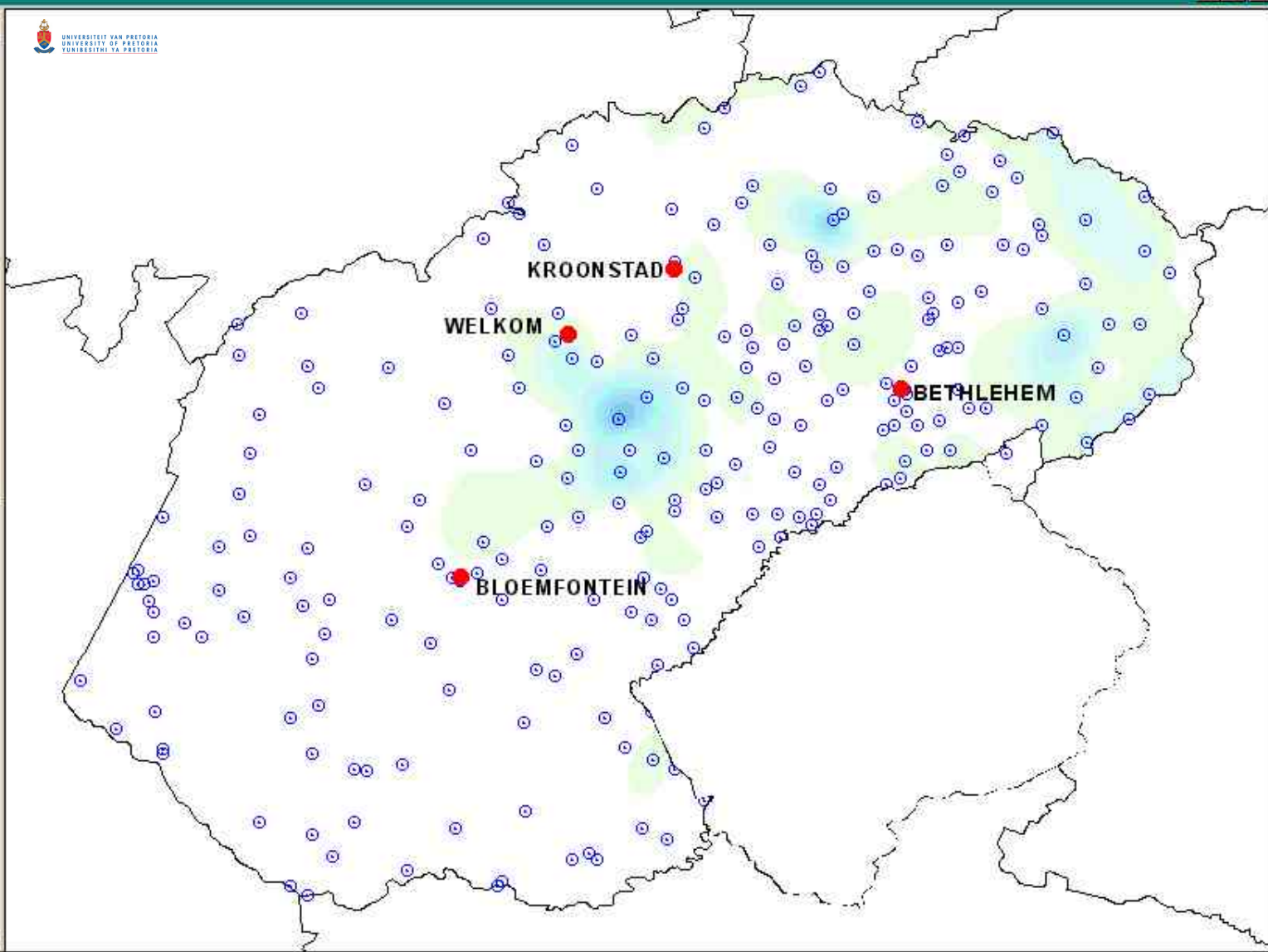


Scale 1: 3,086,181

27.23
-29.28

View1

- 19990 119
- 19990 118
- 19990 117
- 19990 116
- 19990 115
- 19990 114
- 19990 113
- 19990 112
- 19990 111
- 19990 110
- 19990 109
- 19990 108
- 19990 107
- 19990 106
- 19990 105
- 19990 104
- 19990 103
- 19990 102
- 19990 101
- 19981 231
- 19981 230
- 19981 229
- 19981 228
- 19991 227
- 19981 226
- 19981 225
- 19981 224





Scale 1:3,086,181

24.81
-27.57

- 19990 131
- 19990 130
- 19990 129
- 19990 128
- 19990 127
- 19990 126
- 19990 125
- 19990 124
- 19990 123
- 19990 122
- 19990 121
- 19990 120
- 19990 119
- 19990 118
- 19990 117
- 19990 116
- 19990 115
- 19990 114
- 19990 113
- 19990 112
- 19990 111
- 19990 110
- 19990 109
- 19990 108
- 19990 107
- 19990 106
- 19990 105

